5-2018

A Forensic Investigation into the Possible Origins of Three Human Skeletons

Jefferson P. Sinnott
sinnotjp01@mail.buffalostate.edu

First Reader
M. Scott Goodman, Ph.D., Professor of Chemistry
Second Reader
Melanie M. Mayberry, Ph.D., Lecturer in Anthropology
Third Reader
Douglas A. Ridolfi, M.S., Lecturer in Chemistry and Coordinator of Forensic Chemistry Programs
Department Chair
M. Scott Goodman, Ph.D., Professor of Chemistry

A Forensic Investigation into the Possible Origins of Three Human Skeletons

by

Jefferson P. Sinnott

An Abstract of a Thesis
in
Forensic Science

Submitted in Partial Fulfillment
of the Requirements
for the Degree of

Master of Science

May 2018

State University of New York
College at Buffalo

Abstract

A Forensic Investigation into the Possible Origins of Three Human Skeletons

The Anthropology Department at Buffalo State has three human skeletons that have been part of the department's collection for several years. The origin of the skeletons is currently unknown. Modern DNA techniques coupled with forensic anthropological techniques may now allow us to determine with some certainty the geographic origin of the skeletons. Ancestry, sex, age, and stature were assessed using current anthropological techniques. Afterwards, one tooth from each of the three skeletons was extracted, pulverized and DNA was isolated. Y-STR fragment size analysis of the DNA samples can provide information about the patrilineage of male individuals. Mitochondrial DNA sequencing analysis can provide information about the matrilineage of the individuals. All of the individuals appear to be two males and one probable female of Eurasian ancestry, ranging in stature from 5'3" to 5'8", and all estimated to be over 30 years old at time of death.

State University of New York
College at Buffalo
Department of Chemistry

A Forensic Investigation into the Possible Origins of 3 Human Skeletons

A Thesis in
Forensic Science

By

Jefferson P. Sinnott

Submitted in Partial Fulfillment
of the Requirements
for the Degree of

Master of Science

May 2018

Approved by:

M. Scott Goodman, Ph.D.
Chair and Professor of the Chemistry Department
Chairperson of the Committee
Thesis Advisor

Kevin Miller, Ed.D.
Dean of the Graduate School

THESIS COMMITTEE SIGNATORY

M. Scott Goodman, Ph.D.
Professor of Chemistry
Chairperson of the Committee

Melanie M. Mayberry, Ph.D.
Lecturer in Anthropology
Thesis Advisor

Douglas Ridolfi, M.S.
Coordinator of Forensic Chemistry Program
Lecturer in Chemistry

Acknowledgements

First, I would like to thank Dr. Julie Wieczkowski and the Anthropology Department at SUNY Buffalo State, who requested this project and allowed the necessary extractions and analysis to be performed.

I would like to thank Dr. Scott Goodman who took the time to be chair of my committee, thesis co-advisor, and assist me throughout with instrumentation and DNA analysis. It is greatly appreciated.

I would also like to thank Dr. Melanie Mayberry, who as my thesis co-advisor, allowed me to swing by on a whim for help, and consistently pushed me to better myself. I appreciate your knowledge, support, and positive outlook to help complete this project.

Thank you to Professor Douglas Ridolfi, for taking the time to be on my thesis committee, it is greatly appreciated.

I would like to thank Dr. Amy McMillan and Ms. Jennifer Jackson, who allowed the use of their laboratory's equipment, and frequently provided advice on PCR and sequencing reactions.

Thank you to Anne Marie Sokol for all your assistance that you provided throughout the journey of this research project. Many thanks.

Thank you to all my fellow Graduate Assistants and students, your friendship and support are irreplaceable. Thanks to Matt Pothier, you have put up with my friendship for both Undergraduate and Graduate programs, six years of chemistry fun. Thank you, Elisabeth Barone, for the exciting whirlwind that was Summer 2017 and the resulting friendship.

Thank you to my Buffalo friends and family, especially Meaghan Champney and Justin Phillips. I couldn't ask for better roommates/supporting cast. I wouldn't have made it this far without any of you, family or otherwise, you all have my love.

Thank you everyone.

Table of Contents

List of Figures

Figure **Page Number**

List of Tables

Table **Page Number**

I. Introduction

In the field of forensic science, ancestry analysis is most commonly conducted by forensic anthropologists analyzing skeletal remains. In cases such as mass disasters like the September 11th attacks of the World Trade Center, or archaeological cases like the discovery and analysis of the fate of the Romanov family, a combination of anthropometric and DNA analysis can be employed. Traits such as ancestry, sex, age at time of death, and stature can be determined following forensic techniques. These skeletal estimations can be complemented by DNA analysis to determine matrilineage and patrilineage.

For the research presented in this paper, the Department of Anthropology of SUNY Buffalo State requested a biological assessment of three partial skeletons of individuals of unknown origins. The individuals' remains were purchased by the department at an unknown time, but believed to be in the early 1970's and 80's. Any identifying paperwork regarding these individuals is unavailable to the department.

1.1 Osteological Analysis

Forensic anthropology incorporates most of the techniques originating with the analysis of human skeletal material. The use of anthropometry in the field of forensic science and medicine dates to 1882 when Alphonse Bertillon, a French police expert, invented a system of criminal identification based on anthropometric measurements (1). Human skeletal remains often will reach the forensic anthropologist without any documentation of their biological profile, or their individual ancestry, sex, age, and stature. Literature on skeletal analysis is composed of books and articles describing the development of methods to allow

precise identification of individual traits, research that continues even after a century of intensive study (1-19).

Methods for determining the sex of an individual based upon skeletal remains can be broadly divided into two groups: morphological or "subjective" observations; and metric or "objective" techniques. Size and shape characteristics usually allow for the unambiguous sorting of human from nonhuman bone, even fragmentary material. Due to having incomplete skeletons, the methods selected for the assessment of a biological profile all rely on either the skull or os pubis. Although still frequently damaged by taphonomic processes, these bones show the most variation between populations to allow for the development of a biological profile (2-5)

The determination of sex can appear to be an either/or decision, or in some cases an ambiguous assessment, even if there are only a few skeletal characteristics that allow a scientist to make this assessment (2). The other characteristics; ancestry, age at death, and stature, are not as easily determined. Simple divisions for sorting and categorizing do not exist, and rather the traits are typically assessed by phases and groupings of populations.

1.1.1 Estimation of Sex: Phenice Method

The anthropological analysis for estimating sex from skeletal material in a forensic context is integral for the identification of human remains. According to researchers, such as Spradley and Jantz, the pelvis is regarded as providing the highest accuracy levels for sex determination (5). Although many bones of the skeleton present size-related sexual differences, those of the pelvis usually display marked sex differences in morphology independent of size (6-7).

In 1969, Phenice called attention to three aspects of the pelvis that he felt were especially useful for estimating sex from skeletal remains; the ventral arc, the subpubic concavity, and the medial aspect of the ischio-pubic ramus (8). By using the three traits, Phenice was able to estimate the sex of an individual with an accuracy of 96% (7). These traits are highlighted in **Figure 1**.

The ventral arc refers to a "slightly elevated ridge of bone that sweeps inferiorly and laterally across the ventral surface of the pubis, merging with the medial border of the ischio-pubic ramus" (7). Phenice reported that the ventral arc had only been detected in females. He suggested that whereas males may present a similar ridge, it does not match the above definition when the bone is oriented properly (2). In an experiment by Rogers and Saunders, an accuracy of 86.9% was observed when estimating sex with only the ventral arc (6).

The subpubic concavity refers to a lateral recurve in the dorsal ischio-pubic ramus a short distance below the lower margin of the pubic symphysis. Phenice describes this as a female characteristic, noting, however, that some males display a "slight hint" of the trait (7). Rogers and Saunders report an accuracy of 83.8% when estimating sex with only the subpubic concavity (6).

The ischio-pubic ramus refers to the thin, flat piece of bone connecting the pubis to the ischium (2). Phenice noted that in males, the medial aspect of the ischio-pubic ramus displays a broad, flat surface. In contrast, in females, this area more frequently presents a ridge (7). Rogers and Saunders report an accuracy of 80.0% when estimating sex with only the ischio-pubic ramus (6).

To examine the usefulness of these traits in estimating sex, Phenice examined pelvic bones of 275 individuals from the Terry Collection; all representing adults of known sex. Of the 95 females examined, 43 were of European ancestry and 52 of African ancestry. Of the 180 males, 160 were of European ancestry and 20 of African ancestry. Using the three criteria discussed above, Phenice was able to estimate the sex with an accuracy of 96%, with his procedure being slightly more accurate for females than for males and slightly more accurate for individuals of European ancestry than for those of African ancestry (7).

Many researchers have found the Phenice technique to be useful and it has stimulated additional research. Sutherland and Suchey tested aspects of the Phenice technique on 1284 pubic bones of known sex. Since the pubic bones had been removed from cadavers not all the Phenice features could be easily observed. Using only the ventral arc, they were able to estimate sex with an accuracy of 96% (9).

a)

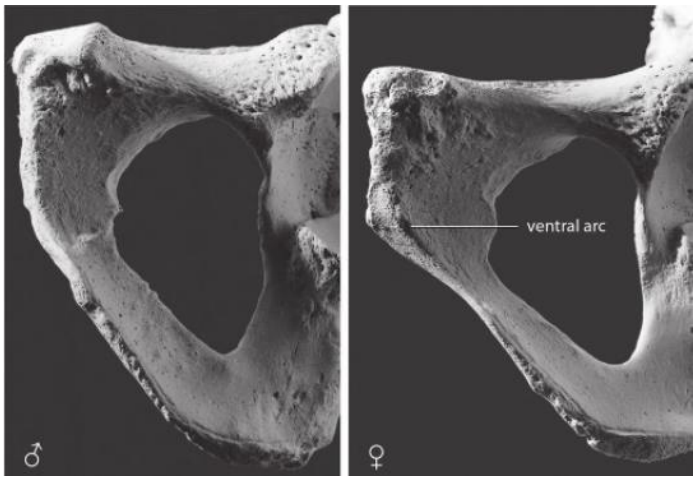

b)

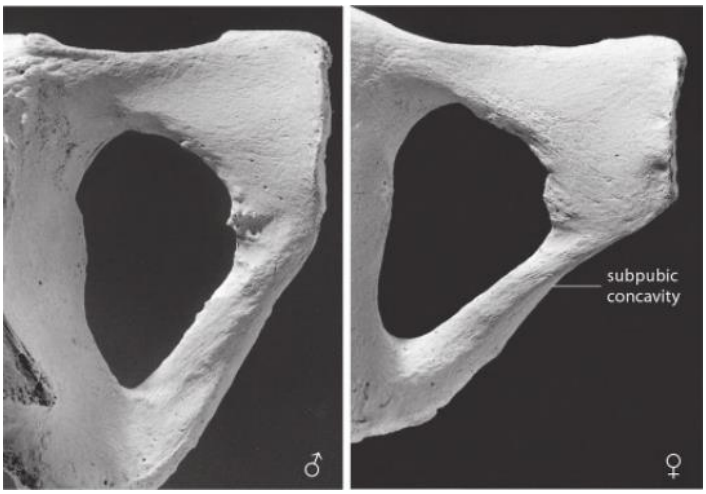

c)

Fig. 1. Images of the pubic regions of 2 human skeletons used in the Phenice method: a) the ventral arc, b) the subpubic concavity, and **c)** the ischio-pubic ramus (2).

1.1.2 Estimation of Sex: Buikstra & Ubelaker Method by Cranial Traits

Not all forensic cases provide the luxury of a complete skeleton. If an individual is left exposed in an outdoor context, taphonomic processes may impede the recovery of skeletal elements. For instance, some cases may consist only of a cranium. In these cases, estimation of sex must be performed using only cranial traits. However, the use of only the cranium is not ideal because these traits are less reliable than estimation by the pubic region.

The expression of sexually dimorphic features of the skull show the greatest relative growth from childhood to adulthood. The growth of female facial features begins to slow around the 13th year of life and maturation is completed soon afterward, while males enter a growth spurt that continues through adolescence with maturation completed in early adulthood. However, since this is a general pattern that varies between individuals, a certain amount of overlap in the size of male and female features is inevitable (10).

Although male skulls are generally larger and have heavier muscle attachments than skulls of females, substantial population-based variation exists. Traits that are sexually dimorphic in one population may be much less so in another. Therefore, standards of skeletal material were used to create a set of recommended methods for documenting adult sexually dimorphic skeletal features. One of the objectives was to devise a simple system that produced comparable results when used by different scientists (11). The cranial traits, detailed in Buikstra and Ubelaker, included the nuchal crest, mastoid process, glabella/supraorbital area, supraorbital margin, and mental eminence **(Figure 2)**.

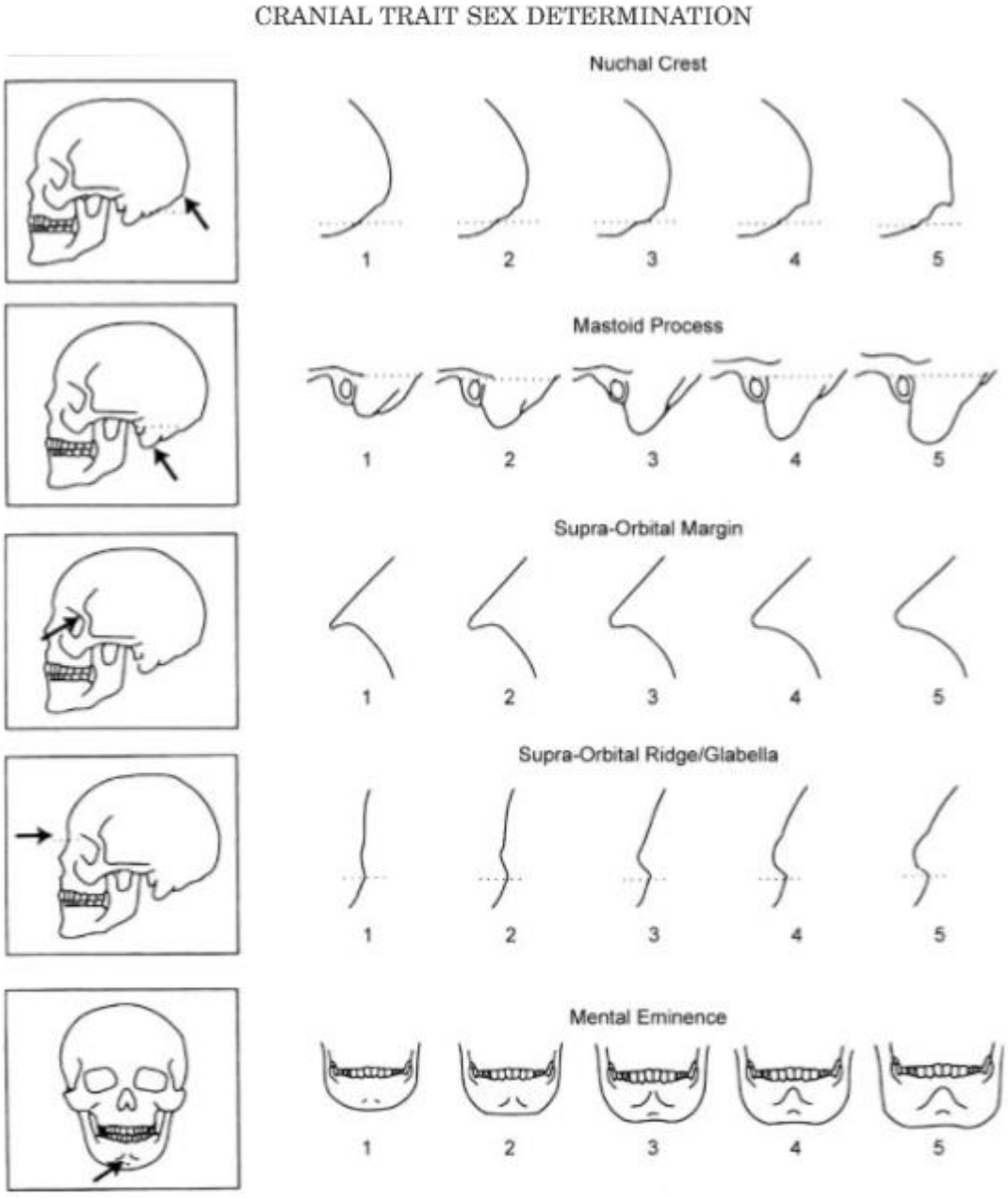

Fig. 2. Standard for scoring cranial traits from Buikstra and Ubelaker. The numbers below each example are the scores to be assigned to specimens whose morphology most closely resembles the condition illustrated. 1 is considered to be feminine and a score of 2 is probable female, while 5 is considered to be masculine and 4 is probable male. A score of 3 is considered to be ambiguous (2).

1.1.3 Estimating Age at Death: Suchey-Brooks Method by Pubic Symphysis

The estimation of the age of adult skeletons is still a continually-developing area in forensic and archaeological fields. Adult age estimates are based on "wear and tear" indicators such as skeletal degeneration and dental and bone remodeling. Most indicators of age have been tested using various skeletal collections of known age (13).

Age estimation depends in part on the skeletal elements available for analysis; different bones are more resilient to damage caused by various taphonomic processes. As a result, there is some bias based on preservation. Sex and population specificity are also important for determining age at death. Because male and female growth trajectories diverge, many current aging standards, which were formulated using standard reference samples, provide separate data for the two sexes (3).

Age estimation based on changes in the pubic symphyseal face has been a long-favored technique. Among the earliest to develop a protocol for scoring degenerative changes in the pubic symphysis was Todd (14). A 10-phase system, Todd's standards remained unchanged until research performed by Brooks provided an updated system (3). Due to the apparent limitations, Suchey and Brooks assembled a set of standards from a large sample amassed between 1977 and 1979 from individuals autopsied the Office of the Chief Medical-Examiner, County of Los Angeles. This sample, which contained 739 male samples and 273 female samples, included demographic information and medical history (15). This resulted in a new series of pubic standards that incorporated a focus on the total pattern of the symphyseal face and degradation of the surface with age (**Figure 3**). Estimations are based on characteristics including billowing/smooth/finely-grained surface, the development of ridges, and rim erosion. Using this system requires the comparison to six-phase sex-specific

reference standard, according to age-related osteological features common to both males and females, for which the mean age and standard deviation of each phase are given by sex (**Table 1**).

Fig. 3. The Suchey-Brooks pubic symphysis scoring system of the six stages (2).

Table 1.

Statistics for the Suchey-Brooks phases in females and males. (2).

	Female (n=273)			Male (n=739)		
Phase	Mean	95% Range	Standard Dev.	Mean	95% Range	Standard Dev.
1	19.4	15-24	2.6	18.5	15-23	2.1
2	25.0	19-40	4.9	23.4	19-34	3.6
3	30.7	21-53	8.1	28.7	21-46	6.5
4	38.2	26-70	10.9	35.2	23-57	9.4
5	48.1	25-83	14.6	46.6	27-66	10.4
6	60.0	42-87	12.4	61.2	34-86	12.2

1.1.4 Estimating Age at Death: Lovejoy Protocol by Auricular Surface

Along with the pubic symphysis, the auricular surface of the ilium is one of the most common locations used for the assessment of age at death. The original standards for estimating skeletal age at death from the auricular surface of the ilium were developed by Lovejoy *et al*. using archaeological samples from the Libben collection, American cadaver collections from the early twentieth century from the Hamann-Todd collection, and forensic cases from the Cuyahoga County Coroner's Office (4,16).

Age changes in the auricular surface are relatively well-defined and sufficiently regular to provide accurate estimates of age at death, though they are somewhat more difficult to interpret than those used for pubic symphyseal aging (16). In burial contexts, the auricular surface often preserves better than the pubic symphysis and the morphological

changes continue well into the sixth decade of life. However, validation studies have shown that the auricular surface method suffers from problems with replicability (4,17).

The changes on the auricular surface due to aging, unlike those on the pubic symphysis, extend well beyond the age of 50. Lovejoy describes age-related changes to the auricular surface, listed in **Table 2**, that include changes in surface granulation, microporosity, macroporosity, transverse organization, billowing, and striations. As age increases, granularity coarsens, and the appearance of billowing and striations reduces dramatically. In the later stages of life, the surface becomes increasingly dense and irregular, losing all evidence of transverse organization (2,16). Examples of these morphological changes are shown in **Figure 4**.

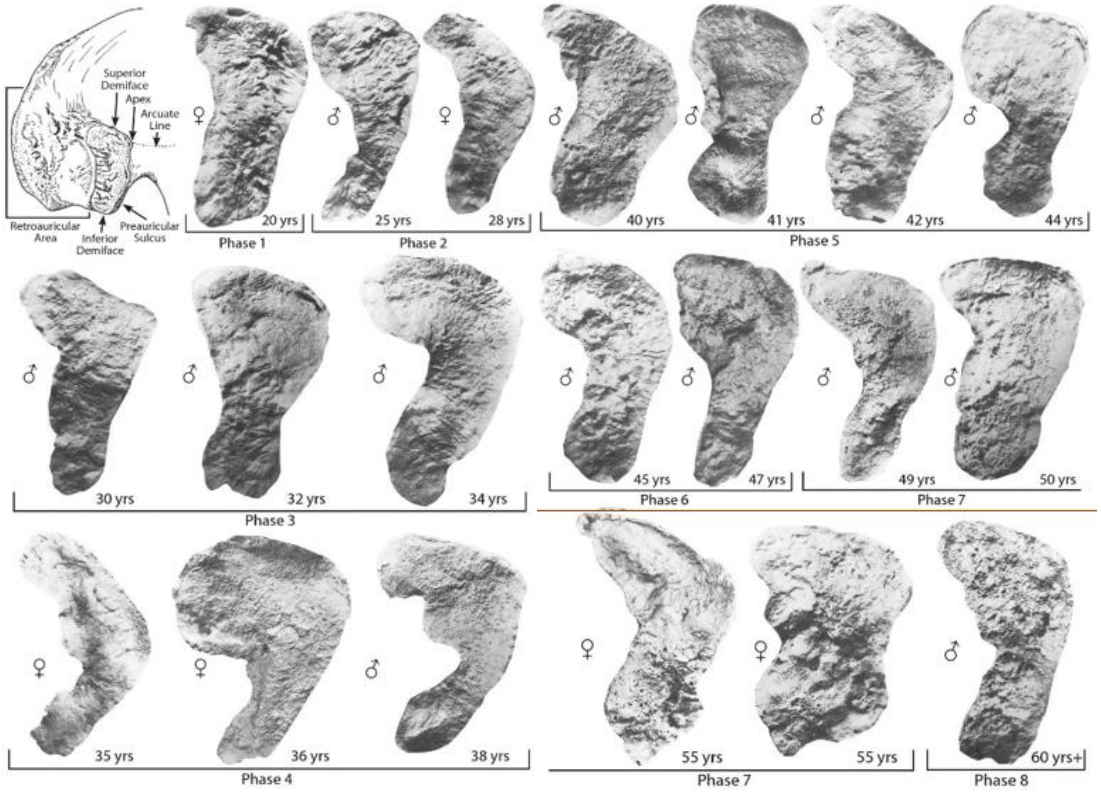

Fig. 4. Modal changes to the auricular surface, as described by Lovejoy. Phases are further described in **Table 2** (2).

Table 2.

The assessment of skeletal age, with provided descriptions for each highlighted phase from **Figure 4**, as described by Lovejoy (2).

Phase	Age Range	Description
Phase 1	20-24	Billowing and very fine granularity
Phase 2	25-29	Reduction of billowing but retention of youthful appearance
Phase 3	30-34	General loss of billowing; replacement by striae, coarsening of granularity
Phase 4	35-39	Uniform coarse granularity
Phase 5	40-44	Transition from coarse granularity to dense surface; this may take place over islands on the surface
Phase 6	45-49	Completion of densification, with complete loss of granularity
Phase 7	50-59	Dense irregular surface of rugged topography and moderate to marked activity in periauricular areas
Phase 8	60+	Breakdown with marginal lipping, microporosity; increased irregularity, and marked activity in periauricular areas

1.1.5 Estimation of Stature

Reconstruction of stature by way of measuring long bones has an established practical application in forensic identification. Although a variety of bones have been used to estimate stature, the most reliable results are based on long bone lengths and particularly the bones of the lower limbs (18). The correlation between bone length and stature is imperfect in living populations and varies between populations. Based on the studies of individuals of known statures, researchers derived regression formulae to estimate stature (19,20).

Trotter and Gleser developed their formulae for estimating male stature based on individuals killed in World War II and the Korean War, whose remains were brought by the American Graves Registration Service, which allowed long bones to be measured prior to

final burial. Female equations were derived from the Terry collection. Their formulae were divided based on "racial" groups and sex, when applicable (**Table 3**) (2,21).

Table 3.

Equations used to estimate stature, in centimeters, with standard error, from the long bones of various groups of individuals (2,22).

White Males [a]		Black Males [a]	
3.574 x Hum + 57.21	± 5.71	3.277 x Hum + 65.46	± 5.72
4.525 x Rad + 61.22	± 5.70	4.235 x Rad + 63.46	± 5.07
4.534 x Uln + 53.33	± 5.66	3.979 x Uln + 62.95	± 5.79
2.701 x Fem + 48.10	± 5.12	2.455 x Fem + 56.66	± 4.84
2.891 x Tib + 62.95	± 5.06	2.455 x Tib + 7548	± 5.03
2.832 x Fib + 66.96	± 5.15	2.665 x Fib + 69.39	± 4.53
White Females [a]		Black Females [a]	
2.534 x Hum + 86.62	± 5.32	3.785 x Hum + 47.35	± 4.56
3.530 x Rad + 83.29	± 4.81	3.781 x Rad + 75.20	± 5.01
3.346 x Uln + 82.82	± 4.51	3.285 x Uln + 80.70	± 4.18
2.624 x Fem + 49.26	± 3.58	2.449 x Fem + 54.86	± 4.34
2.351 x Tib + 80.11	± 4.26	2.855 x Tib + 58.20	± 3.83
2.487 x Fib + 76.51	± 4.16	2.993 x Fib + 55.83	± 4.29
East Asian Males [b]		Hispanic Males [b]	
2.68 x Hum + 83.19	± 4.25	2.92 x Hum + 73.94	± 4.24
3.54 x Rad + 82.00	± 4.60	3.55 x Rad + 80.71	± 4.04
3.48 x Uln + 77.45	± 4.66	3.56 x Uln + 74.56	± 4.05
2.15 x Fem + 72.57	± 3.80	2.44 x Fem + 58.67	± 2.99
2.40 x Fib + 80.56	± 3.24	2.50 x Fib + 75.44	± 3.52

a) Data for White and Black ancestral groups from Wilson *et al.* (2010).
b) Data for Asian and Hispanic ancestral groups from Trotter (1970).

1.1.6 Assessing Ancestry: FORDISC 3.1

Ancestry estimation, or estimation of familial origin, is most commonly accomplished through statistical analysis of measurements from the cranium. This metric analysis relies on the identification of defined landmarks on the skull. Twenty-four cranial and nine mandibular measurements are in use today based on the fact that they represent the overall craniofacial complex and are referred to as inter-landmark distances (ILDs) (23). ILDs are commonly employed by forensic scientists to aid in the creation of the biological profile, especially for the estimation of ancestry using the program FORDISC 3.1. The 24 cranial measurements are listed in **Table 4**.

FORDISC 3.1 is a discriminant function analysis program that contains craniometric data from recent population groups and uses standard, well-defined measurements for the estimation of ancestry (24). The program has a user-friendly interface where measurements from an unknown skull are entered into the program and Discriminant Function Analysis is performed for comparison to reference groups. FORDISC 3.1 is arguably the most widely used program for ancestry estimation, with the authors of the program striving to continually update the Forensic Data Bank (FDB) samples with current reference data (25). The FDB has over 2400 cases, which includes extensive demographic information for many cases, including place of birth, medical history, occupation, stature, and weight. The skeletal information for cases includes cranial and postcranial metrics, various aging criteria scores, and non-metric cranial information (24).

FORDISC relies on metric analysis of cranial features in order to develop an ancestral profile. By using these physical characteristics, the data represents a form of 'racial' ancestry.

This cannot be directly compared to ancestry developed using mitochondrial DNA, since a biological race does not exist.

Table 4.

List of the 24 cranial measurements used in the FORDISC 3.1 program corresponding with **Figure 5**.

Maximum Cranial Length (GOL)	Nasal Height (NLH)
Maximum Cranial Breadth (XCB)	Nasal Breadth (NLB)
Bizygomatic Breadth (ZYB)	Orbital Breadth (OBB)
Basion-Bregma Height (BBH)	Orbital Height (OBH)
Cranial Base Length (BNL)	Biorbital Breadth (EKB)
Basion-Prosthion Length (BPL)	Interorbital Breadth (DKB)
Max. Alveolar Breadth (MAB)	Frontal Chord (FRC)
Max. Alveolar Length (MAL)	Parietal Chord (PAC)
Biauricular Breadth (AUB)	Occipital Chord (OCC)
Upper Facial Height (UFHT)	Foramen Magnum Length (FOL)
Minimum Frontal Breadth (WFB)	Foramen Magnum Breadth (FOB)
Upper Facial Breadth (UFBR)	Mastoid Height (MDH)

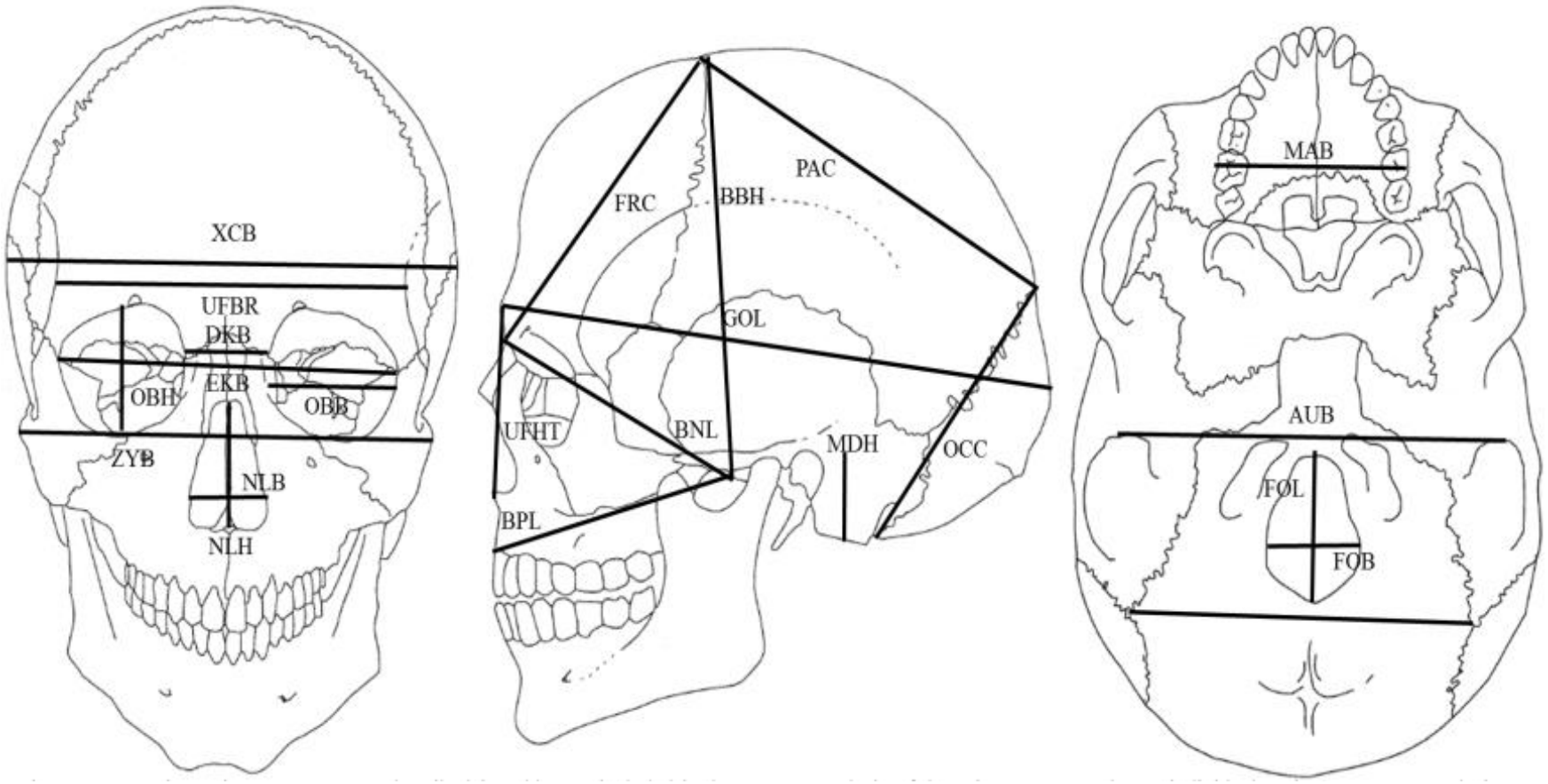

Fig. 5. Cranial measurements, as described in **Table 4**, included in the ancestry analysis performed with FORDISC 3.1 (11 in 12).

1.2 Skeletally Isolated DNA

In forensic investigations, skeletal remains can be amongst the most challenging for genetic DNA analysis. Factors such as temperature, humidity, pH and geochemical properties of the soil and the presence of microorganisms affect the preservation and contamination of the DNA in skeletal remains (26,27). However, archaeological samples as old as 130,000 years old have had water-soluble DNA successfully extracted and analyzed (28). In many forensic cases, teeth and bones are the only potential source of genetic material, and for genetic identification, must be able to supply sufficient amounts of high-quality DNA.

Teeth are among the hardest substances in the human body and have been known to survive diverse postmortem circumstances, due to the structure of enamel. These circumstances can include, but are not limited to, decomposition, submersion in water, burial, and fire damage. The tooth provides an ideal source of DNA, since the pulp is protected from external agents by resistant tissues that protect DNA from degradation (29). As reported by Hildebrand and Sweet, who analyzed extracted molars for DNA yield, the average molar can yield 30.9 µg of DNA material, with a mean concentration of 18.4 µg/mg of powdered tooth. However, the yield of DNA from human teeth is highly variable. The reported amount of DNA ranged from a minimum of 0.5 µg to a maximum of 97.5 µg (30).

Other than the enamel, DNA can be extracted from almost all types of dental tissue; however, the pulp provides the preferred location where the quantity is greatest due to the pulp cavity containing nerve and blood vessels (29). The relative size of the dental pulp is approximately proportional to the relative size of individual classes of teeth. Therefore, molars typically are better sources of pulpal DNA than incisors.

Several methods to access the DNA of human teeth have been used. Among them include vertical cross-sections, horizontal cross-sections, use of a mortar and pestle to crush the teeth (31), and the use of a freezer mill to cryogenically grind the tooth (30). Once both mitochondrial and nuclear DNA isolates have been successful, the samples can potentially be used for examining both maternal and paternal ancestry.

1.2.1 Mitochondrial DNA Analysis

Mitochondrial DNA (mtDNA) is a 16,569 base pair sequence that, because it is inherited solely from the mother and does not recombine (32), makes mtDNA vital for the determination of maternal lineage. Of the entire sequence of mtDNA, the most important for this investigation is the 1,122 base pair long control region commonly referred to as the D-loop (**Figure 6**). This region is the most rapidly-evolving and polymorphic region in the human mtDNA genome (32,33). The D-loop is further divided in the Hyper Variable Region I (HVRI) and Hyper Variable Region II (HVRII). HVI and HVII regions seem to have similar evolutionary processes; however, HVI and HVII show different mutation rates. It also seems that mutation rates are more heterogeneous across nucleotide positions in HVII than in HVI (34).

The first complete sequence of human mtDNA, the Cambridge reference sequence (CRS), was published in 1981, and has since been revised (rCRS) (35). Recently, the interest for human and evolutionary genetics has been in point mutations, also known as single nucleotide polymorphisms (SNPs) (36). In human population studies, the analysis of this variability allows scientists to infer the history of human evolution and patterns of migration. In forensic science, polymorphisms of the mitochondrial DNA genome have been reported as

useful for identity testing and, in general, for the analysis of degraded material, or for samples containing little or no genomic DNA (37).

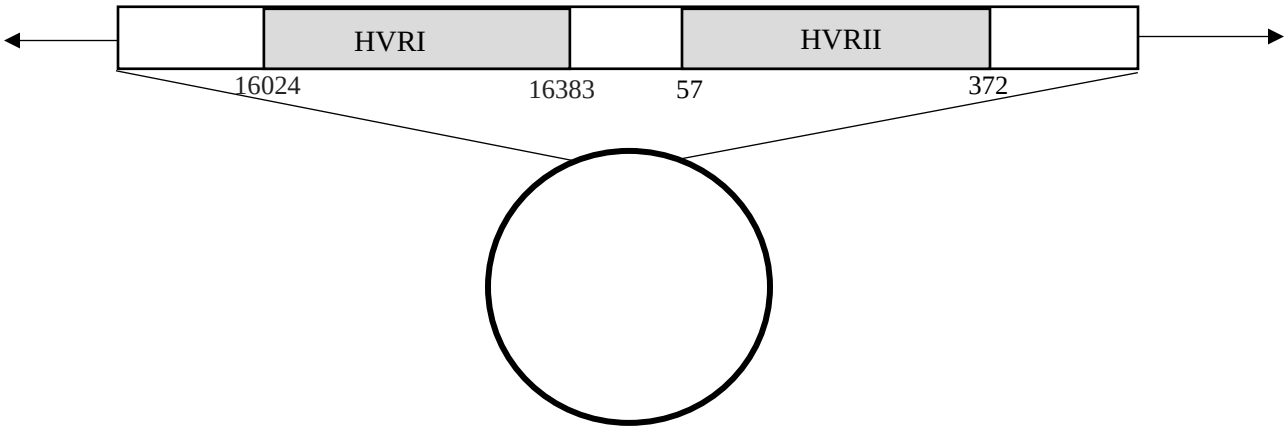

Fig. 6. The human mtDNA control region. The circle represents the circular mtDNA genome. Highlighted is the non-coding, or control, region, which includes HVRI, ranging from base 16024-16383, and HVRII, which ranges from base 57-372.

These polymorphisms define unique haplotypes that are passed from parent to offspring. Similar haplotypes that share a common ancestor with a SNP mutation can then be grouped into a haplogroup. For mitochondrial DNA, all letters of the alphabet except for O have been used to define haplogroups. Haplogroups based on control region sequences by use of informative SNPs can be sorted geographically, depending on the quality and availability of phylogenetic information (38,39).

Haplogroups A, B, C, and D were the first mtDNA haplogroups to be recognized and labelled (40,41). Subsequently, each of these haplogroups has also been found in East Asia, along with haplogroups CZ, D4 and G (within M), and A and N9 (within N) broadly characterize most of the mtDNA lineages found in Northeast Asian populations; while

haplogroups E and M7 (within M) and B4a and R9 (within N) are largely concentrated in populations of continental and island Southeast Asia (41,42).

Virtually all European mtDNA lineages can be classified within the framework of six haplogroups: N1, N2, X, pre-HV, JT, and U, whose distribution is restricted largely to West Eurasia and North Africa. Haplogroups N1, N2, X derive directly from the root of haplogroup N and have a minor frequency throughout Europe. The other three haplogroups, pre-HV, JT, and U, that derive from haplogroup R, cover altogether approximately 80–90% of the total variation in most European populations (41).

The root of the mtDNA phylogeny and the most diverse branches are restricted to African populations. Enabled by the analysis of whole mtDNA genomes, the first seven bifurcations of the phylogenic tree define the distinction of strictly sub-Saharan African branches (L0-L6) (41,43). All these branches con be combined to form a phylogenic map (**Figure 7**). Based on the SNPs observed in an individual's HVRI and HVRII, a rough placement for individuals whose mtDNA has been sequenced can be made onto the following map.

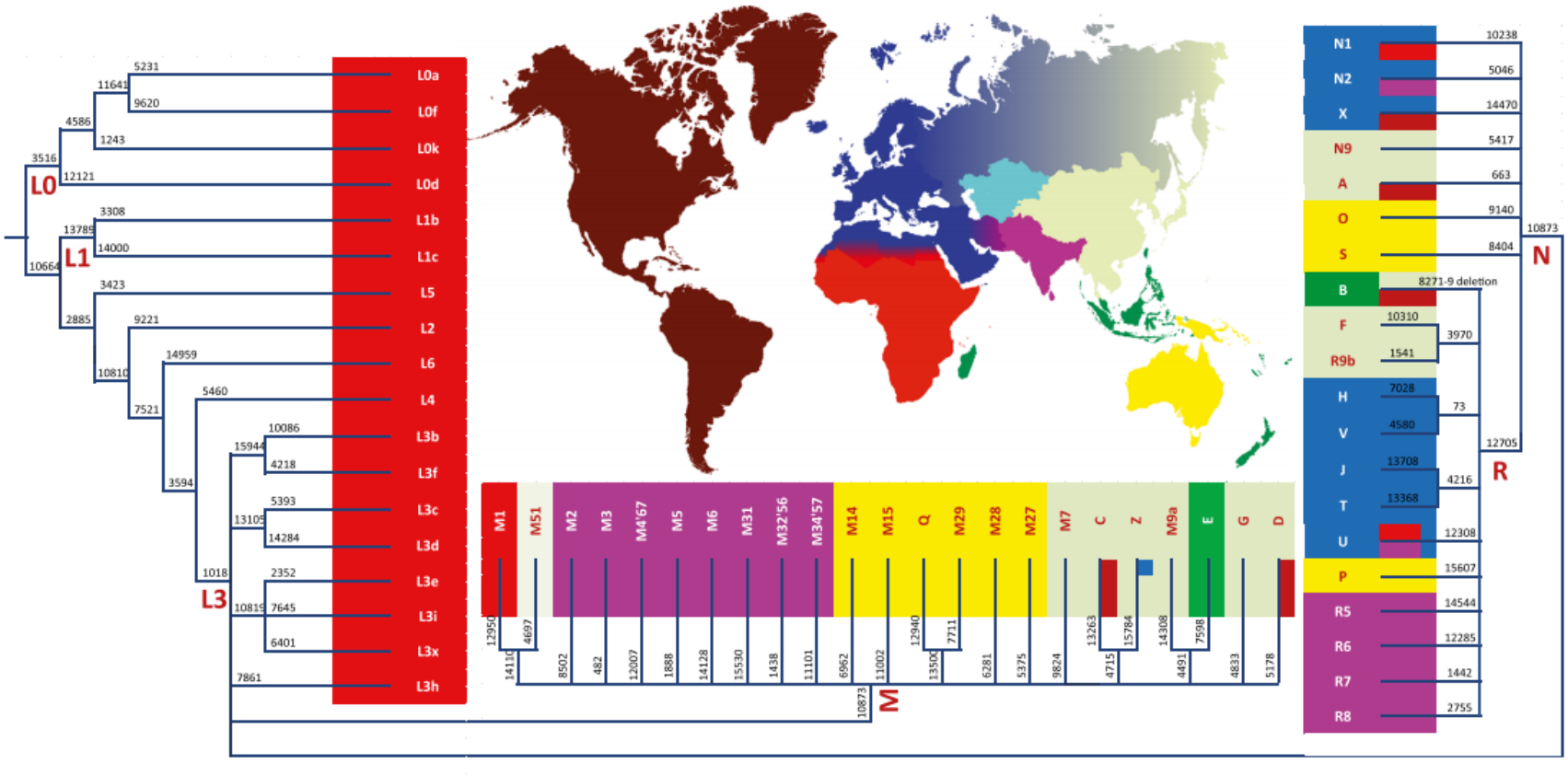

Fig. 7. Image depicting mtDNA haplogroup tree and distribution throughout the world. The main geographic features of haplogroup distribution are separated by color (44).

1.2.2 Y-Chromosome Ancestry

Although Y Chromosome DNA can be analyzed for SNPs, Short Tandem Repeats, or STRs (**Figure 8**) can also be used. STRs are segments of repeated DNA with repeat lengths of up to about 6 basepairs and with total lengths usually less than 60 basepairs. Hundreds of thousands of STRs are interspersed throughout mammalian genomes. In the human Y-chromosome, due to the haploid and non-recombining nature of Y-chromosomal DNA, STRs can be used for male identification purposes (45,46).

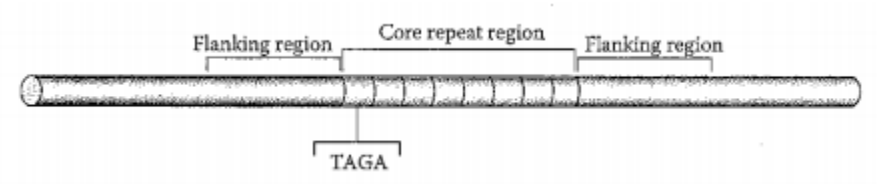

Fig. 8. Core repeat and flanking regions of an STR loci. It consists of 8 repeating units of tetrameric nucleotides (TAGA); thus, it is designated as allele 8 (47).

Due to the sensitivity of Y-chromosome-specific STRs for population differentiation, one global database was created to reflect the Y-chromosomal landscape: the Y Chromosome Haplotype Reference Database (YHRD). The database currently has seven major populations defined: Eurasian, African, Afroeurasian, East Asian, Amerindian, Australian Aboriginal, Eskimo Aleut, as well as an admixed population. These populations are divided further into twenty subgroups (48). These populations and subgroups can be observed in **Figure 9**.

Six subgroups exist for the Eurasian population: European, Altaic, Caucasian, Uralic, Indo Iranian, and Indian. One of these subgroups, the Europeans, has been differentiated further according to genetic analysis (Western, Eastern and Southeastern Europeans). East Asian, the largest of the major populations, is divided into eight subgroups: Korean, Japanese, Sino Tibetan, Austroasiatic, Thai, Austronesian, Indo Pacific, and Dravidian. The

African population is divided into three subgroups: Subsaharan, Afro-American, and Afro-Caribbean, and the population Afroeurasian is also split into three subgroups: Semitic, Berber, and Cushitic.

Through the use of Y-STRs, genealogical relationships between two or more males can be observed for immediate paternal relations, and global clusters of similar STR profiles can be observed for popular analysis. In order to observe a group or family of Y-chromosomes related beyond immediate paternal relations, SNPs on the Y-chromosome can be analyzed. This data can result in the development of Y-chromosome haplogroups (49). However, Y-haplogroups can be predicted by comparing an individual's Y-STR haplotype to individuals of known STR haplotypes and haplogroups (49,50), an option provided by YHRD.

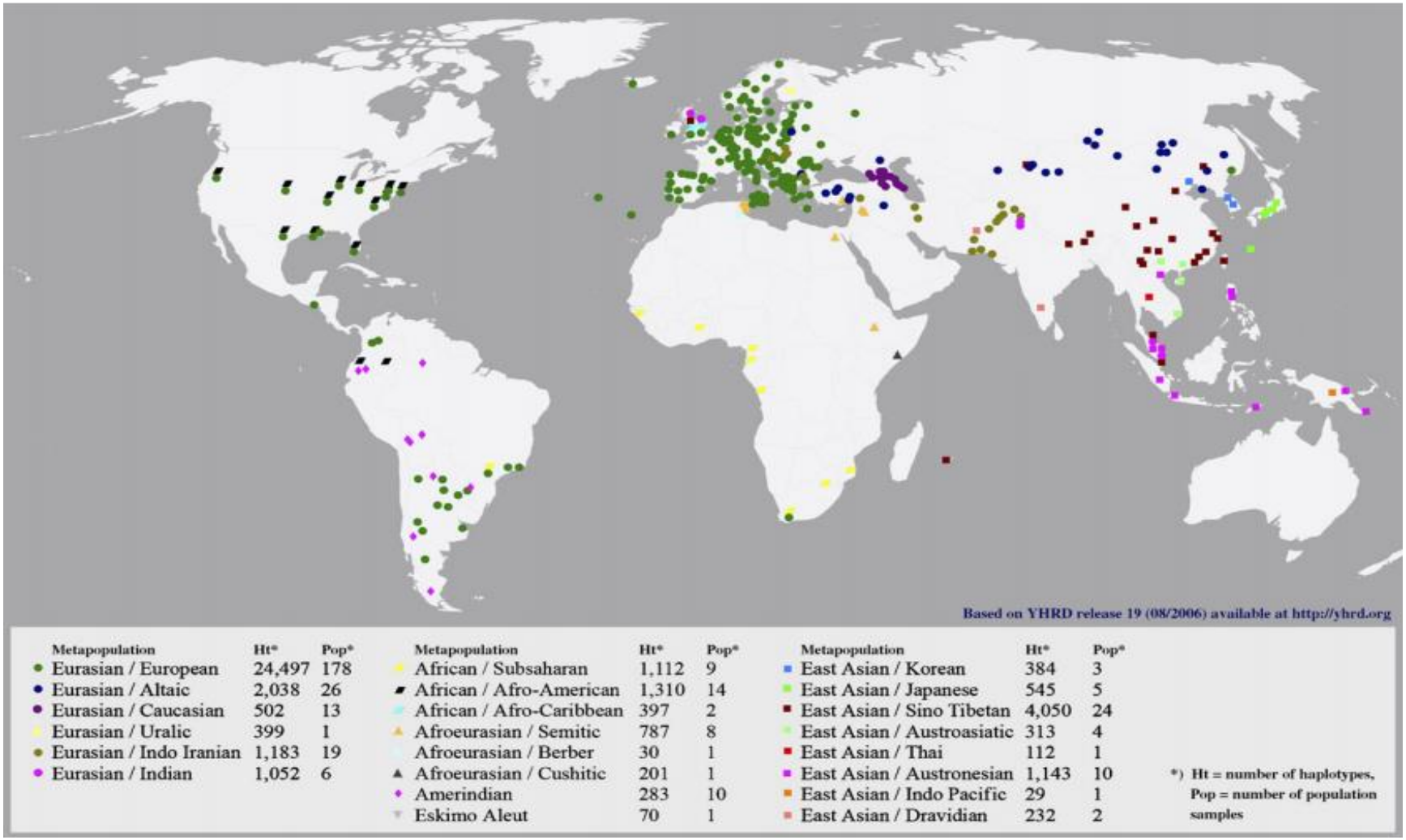

Fig. 9. Worldwide distribution of metapopulations based on YHRD release 19 (August 2006). Haplotypes are defined as an individual YSTR profile, while population is defined as a group of haplotypes submitted together that share a common linguistic, demographic, genetic or geographic background. Population samples classified as admixed (1296 haplotypes within 18 populations) were excluded (48).

1.3 Research Objective

The objective of this thesis project is to assess the common forensic anthropological techniques for the development of a biological profile for three sets of skeletal remains. Also assessed was the possibility of extraction of mitochondrial and nuclear DNA from tooth samples extracted from the individuals, which if successful could be used to assess maternal and paternal ancestry. The results can be combined to provide a background for the three individuals stored by the Anthropology department at SUNY Buffalo State.

.

II. Methods and Materials

2.1 Biological Profile

For this thesis project, the Anthropology department at SUNY Buffalo State provided three individuals for analysis. These individuals either have structural abnormalities, including fused or damage bones, or are incomplete. **Table 5** lists the numerical label found on all bones for each individual, and an approximate percentage of how much of the skeleton was available for use. For this paper, Individual 73-02053 will be referred to as Individual A, Individual 73-02056 will be referred to as Individual B, and Individual 8339 will be referred to as Individual C. All data collection was performed by the same researcher two times, with 3 weeks between trials to account for data reliability.

Table 5.

List of individuals assessed, along with approximate completeness of skeleton

	Numerical Label	**Amount of Skeleton Available**
A	73-02053	60%
B	73-02056	60%
C	8339	90%

2.1.1 Estimation of Sex: Phenice Method

Pubic bones of the three individuals were isolated from the skeletons for analysis. Individuals A and B both only have half of the pelvis. Individual A has a right os coxa available, while Individual B has a left os coxa available. Individual C has the full os coxae available, and the right os coxa was selected for analysis.

Without any knowledge regarding the individuals, the sex of the individuals was estimated following the Phenice technique traits described in **Figure 1**.

2.1.2 Estimation of Sex: Buikstra & Ubelaker Method by Cranial Traits

Each individual's skull was examined for sex estimation based on cranial traits. The traits analyzed were those detailed by Buikstra and Ubelaker, detailed in **Figure 2**. Four cranial traits were assessed (nuchal crest, mastoid process, glabella/supraorbital area, supraorbital margin) along with one mandibular trait (mental eminence). Scoring from 1 (female) to 5 (male) was performed as described in **Figure 2** in the Introduction.

2.1.3 Estimating Age at Death: Suchey-Brooks Method by Pubic Symphysis

The same pubis bones of the three individuals isolated for sex estimation were used for estimation of age. For the Suchey-Brooks method, the symphyseal face of the pubis was evaluated. Based on the observed and recorded characteristics of the symphyseal face, a score of 1-6 was assessed (**Figure 3**). The score was then applied to **Table 1**, and a mean and minimum age at death based on the 95% range were assessed.

2.1.4 Estimating Age at Death: Lovejoy Method by Auricular Surface

For the Lovejoy method, the auricular surface of the ilium was evaluated. Based on the observed and recorded characteristics of the auricular surface, a phase of 1-8 was determined (**Figure 4**). The phase was then applied to **Table 2**, and a minimum age at death was assessed based on the provided age range.

2.1.5 Estimation of Stature: Revised Trotter Method using Long Bones

In order to assess stature, measurements were made to the nearest millimeter using a Carolina Osteometric Board. Only the humerus, radius, ulna, femur, and fibula were used for stature assessment to account for the absence of the tibia in the original Trotter equations.

Individual A and B each only have one side of the skeleton available, while Individual C had both sides of each long bone available except for the femur, which only the right was available. Therefore, the right sided option for each long bone was used for Individual C. Measurements from the two trials were averaged and rounded to the nearest tenth of a millimeter before calculating the estimation of stature. The set of equations to use was selected after estimation of ancestry was made using FORDISC 3.1.

2.1.6 Estimation of Ancestry:

Analysis by FORDISC 3.1 followed the protocol detailed Ousley and Jantz (24). Measurements of the skull were made using both a sliding and spreading caliper, which allowed for measurements to the nearest 0.1 cm.

Initial data analysis included all FDB standard populations within FORDISC. Since sex of the individual was uncertain, both sex options were used initially. Afterwards, the least

statistically-likely groups were ruled out, beginning with sex, followed by least-likely racial/ancestral group. All available FORDISC measurements were initially entered into the program, and an assessment was made for the removal of certain measurements. FORDISC requires inputting a limited number of measurements, so measurements that fell outside two standard deviations according to the programs analytics were eliminated immediately. FORDISC provides the estimated likelihood of proper population assignment given the provided measurements, and for this research an assessment of ancestral population was made with a goal of a minimum of 65% likelihood estimate.

2.2 DNA Extraction

2.2.0 General Methods

All DNA isolation was performed using and following the protocols detailed by the PureLink™ Genomic DNA Mini Kit (51).

All DNA quantitation was performed using the Qubit 2.0 Fluorometer and the appropriate reagents following the protocol for the High Sensitivity dsDNA Assay Kit.

Amplification of DNA products for mitochondrial DNA sequencing and nuclear STR profiling was performed on the BioRad T100 Thermal Cycler. PCR conditions and reagents followed the Forensic Biology Protocols for Forensic Mitochondrial DNA Analysis by the NYC Office of Chief Medical Examiner (52). PCR products were analyzed following the protocols for the Agilent 2200 TapeStation System using D1000 ScreenTapes.

PCR products were cleaned following the ExoSAP-IT™ PCR Product Cleanup Reagent protocols prior to DNA sequencing. DNA sequencing was performed following the protocols and using the BigDye Terminator v3.1 Cycle Sequencing Kit (53).

STR analysis was performed using the AmpFlSTR® Identifiler® Plus PCR Amplification Kit using the protocols from the provided user guide (54). Y-STR analysis was performed using the AmpFlSTR® Yfiler® PCR Amplification Kit following the protocols from the provided user manual (55).

All DNA analysis was performed using the 3500 Series Genetic Analyzer (**Figure 10**). POP-7 polymer was used for all sequencing analysis. POP-4 polymer was used for all STR analysis.

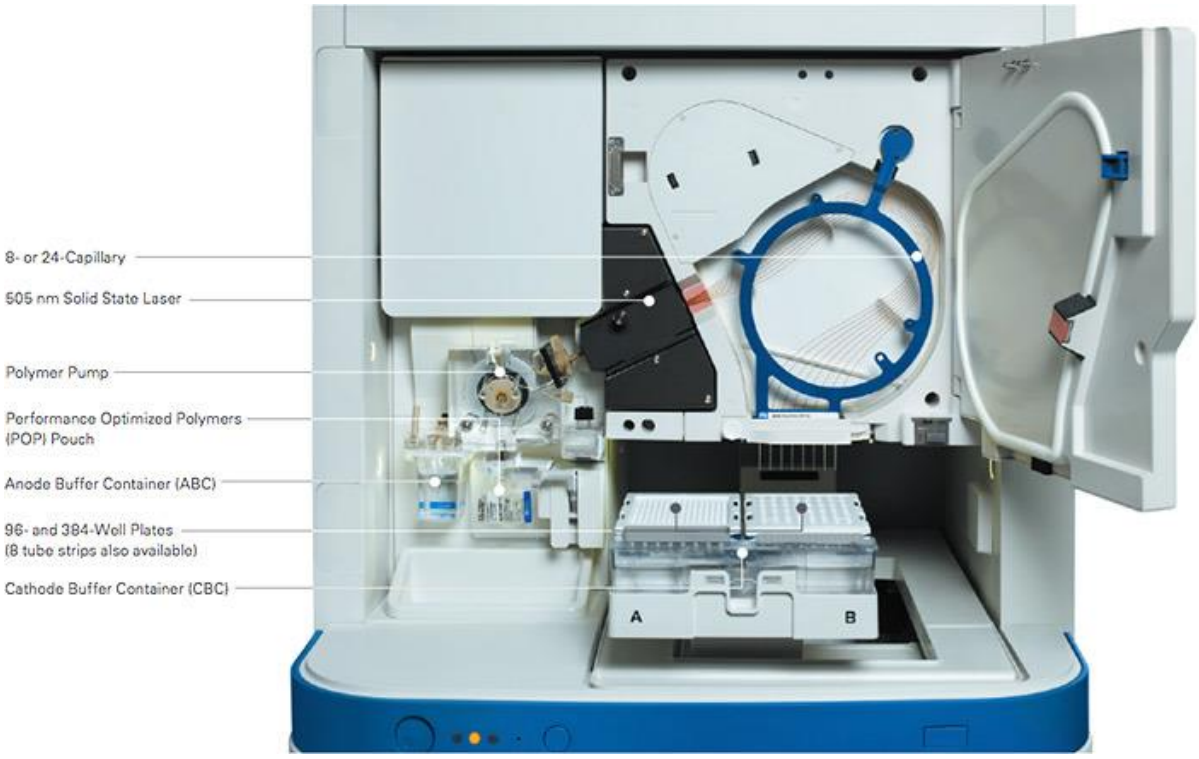

Fig. 10. Schematic of the 3500 Series Genetic Analyzer (Thermo Fisher).

2.2.1 Selection and Destruction of Tooth Samples

From each of the individuals, one molar was selected for DNA isolation. Samples were selected in order to avoid damage to the overall skeleton. Each tooth was rinsed using distilled water to remove particulates. Since DNA contamination is a constant threat when analyzing skeletal DNA (56,57), each tooth was cleaned following a four-step process. Tooth samples were soaked in a detergent/absolute ethanol mixture for a minimum of 5 minutes, followed by brief agitation by vortexing. The tooth samples were then rinsed with a phosphate buffered saline (PBS) solution to remove and remaining detergent solution, followed by a rinse of absolute ethanol to help remove residual PBS solution. Tooth samples were then air dried in a SterilGARD Biosafety Cabinet under ultraviolet (UV) light.

All steps involving the tooth samples were carried out in the SterilGARD Biosafety Cabinet to protect from outside DNA contamination. However, it must be noted that the chemical laboratories at SUNY Buffalo State are not accredited clean labs and are not functionally sterile.

To combat the risk of DNA contamination all equipment was cleaned using a 10% bleach solution, followed by a rinse with 70% ethanol and air dried under UV light.

Negative controls were created by using nuclease-free water in place of DNA samples. A fourth sample, a recently extracted tooth from an anonymous source outside of this research project, was provided for testing to confirm that the extraction protocol was effective and was submitted to an identical procedure. This tooth was labeled MT and will be referred to as such throughout this thesis.

The method of extraction was based on protocols developed by Rohland (58) and Rothe (59). Tooth samples were first crushed by mortar and pestle to obtain smaller fragments for pulverization. Tooth pieces were then made into a fine-grained powder using a Wig-L-Bug grinder equipped with a steel vial and ball pestle that were sterilized using a 10% bleach solution. 250 mg of tooth powder was added to a mixture of 3600 µL of 0.5 M EDTA and 50 µL of 600 mg/mL Proteinase K. The EDTA caused decalcification of the tooth, while the Proteinase K caused lysis of the DNA. This solution was incubated in a water bath at 37˚C with gentle agitation for 18-24 hours.

The only exceptions to this were two attempts to isolate DNA using tooth MT. In these two cases, the incubation temperature was increased to 57 ˚C and incubation was allowed to proceed overnight for 18-24 hours to determine if there was a difference in quantity of isolated DNA at a higher incubation temperature. The DNA isolation protocol continued from this point unchanged.

2.3 Mitochondrial DNA Analysis

Isolates of the mitochondrial DNA sequence were obtained using the forward and reverse primers detailed in **Table 6**. With every PCR reaction performed, a negative blank was assessed to ensure that no exogeneous DNA contamination had occurred. A positive control was run to ensure the primers and PCR set-up were operational.

Completed sequences were compared to the rCRS using the Basic Local Alignment Search Tool (BLAST) from the National Center for Biotechnology Information. Any SNPs were recorded and then compared to the PhyloTree mtDNA Tree Build (38) using the search

program from https://dna.jameslick.com/mthap in order to place individuals into haplogroups, as described in the Introduction.

Table 6.

Details of primers used for analysis of mitochondrial DNA. Positions are detailed in **Figure 37** in the Appendix.

Primer Name	**Position and Direction**	**Primer Sequence 5'-3'**
A1 Primer	F15997	5' CAC CAT TAG CAC CCA AAG CT 3'
A4 Primer	F16209	5' CCC CAT GCT TAC AAG CAA GT 3'
B1 Primer	R16391	5' GAG GAT GGT GGT CAA GGG AC 3'
B4 Primer	R16164	5' TTT GAT GTG GAT TGG GTT T 3'
C1 Primer	F048	5' CTC ACG GGA GCT CTC CAT GC 3'
C2 Primer	F177	5' TTA TTT ATC GCA CCT ACG TTC AAT 3'
D1 Primer	R408	5' CTG TTA AAA GTG CAT ACC GCC A 3'
D2 Primer	R266	5' GGG GTT TGG TGG AAA TTT TTT G 3'

2.4 STR and Y-STR DNA Analysis

STR profiles were completed to compare to researcher profiles to assess the possibility of DNA contamination. The development of an STR profile will also assess the biological sex of the individual. If the individual was determined to be male, then the DNA sample would be analyzed for a Y-STR profile. Y-STR profiles would then be compared to the Y-Chromosome Haplotype Research Database (YHRD) to determine population affinity.

III. Results

3.1 Biological Profile Assessment

3.1.1 Estimation of Sex: Phenice Method

When assessing Phenice's three pubic traits (**Table 7**), two individuals were assessed as male, Individual A and Individual B. Individual C was assessed as female. For Individual A, the ventral arc (**Figure 1a)** and subpubic concavity (**Figure 1b**) are not present, a characteristic found in male samples. The medial aspect of the ischio-pubic ramus (**Figure 1c**) could be considered narrower than is typically seen in male samples, but this alone does not overrule the other assessed traits. For Individual B, the ventral arc and subpubic concavity were not present, while the medial aspect of the ischio-pubic ramus was described as broad, all characteristics found in male samples. For Individual C, the ventral arc and subpubic concavity were present, while the medial aspect of the ischio-pubic ramus was described as sharp and narrow, all characteristics found in female samples.

Table 7.

Assessment of Phenice's three pelvic features for estimating sex. Descriptions of each feature are recorded, along with the overall estimation of sex.

	Pelvic Features			
Individual	**Ventral Arc**	**Subpubic Concavity**	**Medial Aspect of the Ischio-pubic Ramus**	**Estimation of Sex**
A	Is not present	Is not present	Flat, narrow	Male
	Is not present	Is not present	Flat	Male
B	Is not present	Is not present	Flat, broad	Male
	Flat, is not present	Is not present	Flat, very broad	Male
C	Present	Present	Smooth, not strongly present	Female
	Present	Present	Smooth, not present	Female

3.1.2 Estimation of Sex: Buikstra and Ubelaker Method

When assessing Buikstra and Ubelaker's cranial traits (**Table 8**), Individual A was assessed as probable female, Individual B was assessed as male, and Individual C was assessed as probable female. For Individual A, traits such as the Mastoid Process, Mental Eminence, and the Supra-Orbital Ridge appeared gracile and were assessed a 1 or 2. The Nuchal Crest and the Supra-Orbital Margin were assessed a score of 3, which means sex based on these traits is ambiguous. For Individual B, all five traits received a score of 4 or 5, leading to an estimation of sex as male. For Individual C, the Mastoid Process, Nuchal Crest, Supra-Orbital Ridge, and Supra-Orbital Margin all received a score of 1 or 2, leading to an

estimation of sex as female. The Mental Eminence received a score of 3, but this ambiguous score was not enough to overrule the four other assessed traits.

Table 8.

Assessment of cranial features for the estimation of sex. An overall estimation of sex was made by considering the scores of all. Individual A gave the only ambiguous result, observed in the second trial. 1 is most female, 5 is most male.

	Cranial and Mandibular Traits used in Sex Estimation					
Individual	**Nuchal Crest**	**Mastoid Process**	**Supra-Orbital Margin**	**Supra-Orbital Ridge**	**Mental Eminence**	**Estimation of Sex**
A	2	1	2	1	2	Probable Female
	3	2	3	1	2	Ambiguous
B	5	4	4	4	4	Probable Male
	5	5	4	4	4	Male
C	2	2	2	2	3	Probable Female
	2	1	2	1	3	Probable Female

3.1.3 Estimation of Age: Suchey-Brooks Method

Estimation of age was first performed using the Suchey-Brooks method, which assessed the pubic symphysis (**Figure 11**). For each individual, no billowing was present, and granularity was fine in size. For Individual A and Individual B, an outline or ridge was assessed (**Table 9**). These two individuals were both assessed as Phase 4, reporting a mean age of 35 years, with a minimum age of 21 years. Individual C was assessed as Phase 3, reporting a mean age of 31, with a minimum age of 21 years.

Table 9.

Assessment of the characteristics of the surface of the pubic symphysis. Based on features determined by Suchey and Brooks. Based on the scored phase, a mean and minimum age was estimated.

Individual	Visual Assessment and Description	Phase	Mean Age	Minimum Age
A	Finely grained, possibility of some striae, outline complete	Phase 4	35	21
		Phase 4	35	21
B	No billowing present, no striae, rim is present and nearly complete, no depressions, no lipping	Phase 4	35	21
		Phase 4	35	21
C	No billowing or striae, no distinct edge, mostly smooth, granularity developing	Phase 3	31	21
		Phase 3	31	21

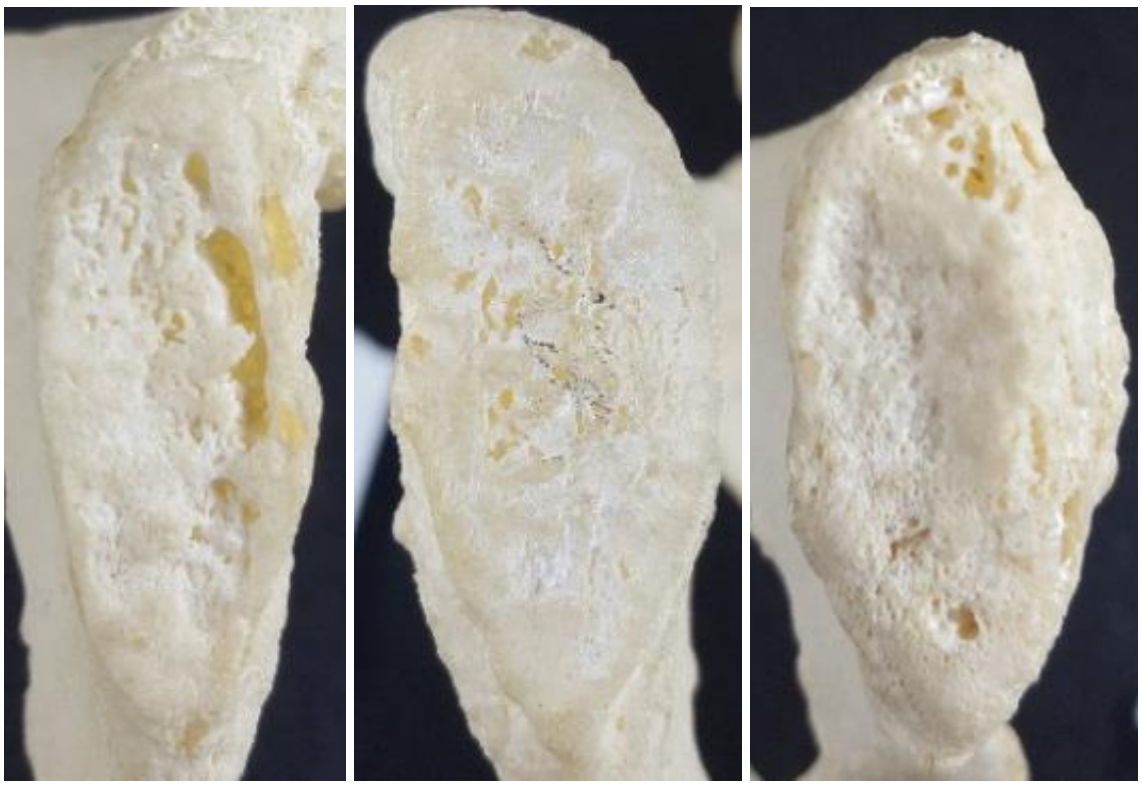

Fig. 11. Pubic symphysis of Individual A (left), B (center), C (right)

3.1.4 Estimation of Age: Lovejoy Method

Estimation of age was then performed using the Lovejoy method, which assessed the auricular surface of the ilium (**Figure 12**). For Individual A and Individual B, no striae or billowing was present, and the surface was finely granular (**Table 10**). It was also reported that densification of the bone was present in one of the trials for Individual B. Individual A was assessed as Phase 4, reporting a minimum age of 35 years, while Individual B was assessed Phase 4 once and Phase 5 once. The minimum age for this individual was estimated at 35 years. Individual C was assessed as Phase 3, reporting a with a minimum age of 30 years.

Table 10.

Assessment of the characteristics of the auricular surface of the ilium. Based on features determined by Lovejoy.

Individual	**Visual Assessment and Description**	**Phase**	**Minimum Age**
A	No present striae or billowing, surface is smooth/finely granular	Phase 4	35
		Phase 4	35
B	No present striae or billowing, granularity present, densification beginning	Phase 4	35
		Phase 5	40
C	Appearance of striae, beginning of granular development	Phase 3	30
		Phase 3	30

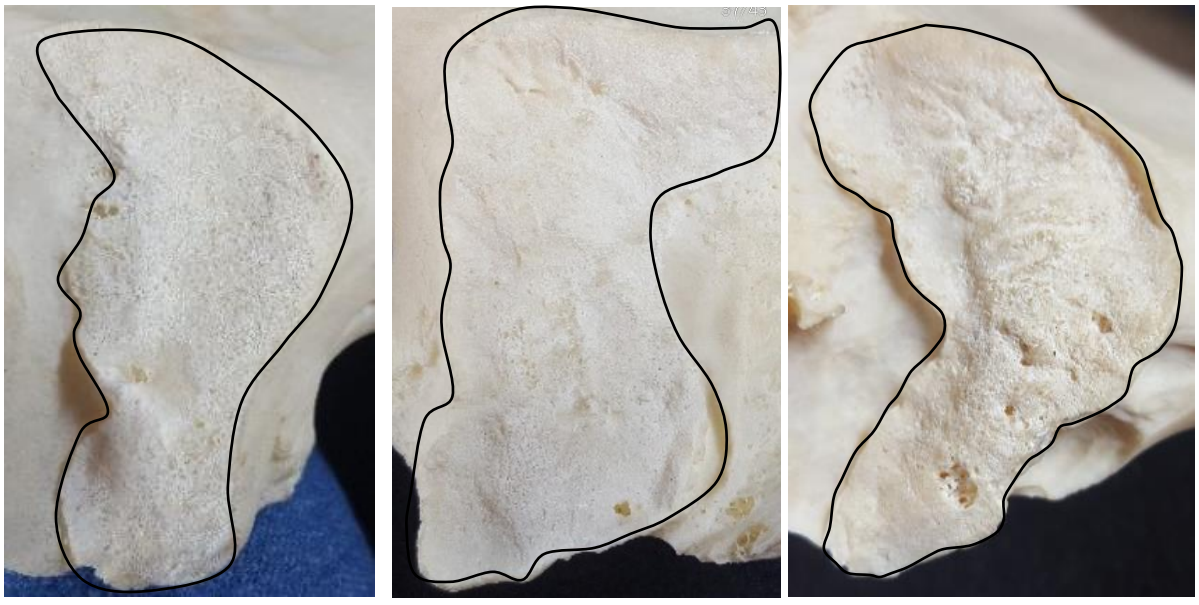

Fig. 12. Auricular surface of the Ilium of the right os coxae Individual A (left), the left os coxae of Individual B (center), and the right os coxae of Individual C (right).

3.1.5 Estimation of Stature: Trotter/Wilson Method

Stature was estimated using the updated set of equations for Caucasian and African individuals edited by Wilson, along with the Hispanic and East Asian equations first created by Trotter. Measurements of the long bones (**Table 11**) were consistent in both trials for all three individuals with a maximum difference of 0.1 cm observed in all trials except for the measurements of the fibula of Individual C, which differed by 0.2 cm. All measurements were averaged and rounded to the nearest 0.1 cm.

For Individual A, the White Male equation set was selected. The stature for Individual A was estimated to be between 5’4” and 5’6.5” with an error of 2 inches. For Individual B, the White Male equation set was selected. The stature for Individual B was estimated to be between 5’6” and 5’8” with an error of 2 inches.

For Individual C, two sets of equations were selected, the White Female set and the East Asian Male set. This was because the ancestry of Individual C was assessed to be East Asian, and sex was estimated to be female. A set of equations for stature estimation of the combination was not created by Trotter or Wilson. The stature of Individual C was estimated to be between 5’2” and 5’5.5” with an error of 2 inches according to the equations for White Females, and an estimated height between 5’3.5” and 5’4.5” with an error of approximately 1.75’ according to the equations for East Asian Males.

Table 11.

Measurements of long bones (humerus, radius, ulna, femur and fibula) for the estimation of stature. Measurements were taken in duplicate to the nearest 0.1 cm.

	Humerus	**Radius**	**Ulna**	**Femur**	**Fibula**
A	30.1	23.2	25.3	42.2	35.9
	30.1	23.1	25.3	42.1	35.9
Stature (cm)	164.8 ± 5.7	166.2 ± 5.7	168.0 ± 5.6	162.1 ± 5.1	168.6 ± 5.2
Stature (ft)	5 ft 4.9 in ± 2.2 in	5 ft 5.4 in ± 2.2 in	5 ft 6.2 in ± 2.2 in	5 ft 3.8 in ± 2.0 in	5 ft 6.4 in ± 2.0 in
B	31.5	24.4	26.2	44.2	36.2
	31.4	24.4	26.2	44.2	36.2
Stature (cm)	169.8 ± 5.7	171.6 ± 5.7	172.1 ± 5.7	167.5 ± 5.1	169.5 ± 5.1
Stature (ft)	5 ft 6.8 in ± 2.2 in	5 ft 7.6 in ± 2.2 in	5 ft 7.8 in ± 2.2 in	5 ft 5.9 in ± 2.0 in	5 ft 6.7 in ± 2.0 in
C	29.1	23.2	24.8	41.2	34.5
	29.1	23.2	24.8	41.1	34.3
Stature for WF (cm)	160.4 ± 5.3	165.2 ± 4.8	165.8 ± 4.5	157.4 ± 3.6	161.6 ± 4.2
Stature for WF (ft)	5 ft 3.1 in ± 2.1 in	5 ft 5.0 in ± 1.9 in	5 ft 5.3 in ± 1.8 in	5 ft 2.0 in ± 1.4 in	5 ft 3.6 in ± 1.6 in
Stature for EAM (cm)	161.2 ± 4.3	164.1 ± 4.6	163.8 ± 4.7	161.1 ± 3.8	162.6 ± 3.2
Stature for EAM (ft)	5 ft 3.5 in ± 1.7 in	5 ft 4.6 in ± 1.8 in	5 ft 4.5 in ± 1.8 in	5 ft 3.4 in ± 1.5 in	5 ft 4.0 in ± 1.3 in

3.1.6 Estimation of Ancestry: FORDISC 3.1

The final part of the biological profile was the estimation of ancestry. The measurements of the twenty-four cranial measurements were recorded in **Table 12**. The two trials were averaged before being input into FORDISC. For Individual A, the Basion-Prosthion length showed the largest change between trials at 9 mm, and was eliminated from FORDISC analysis immediately, while the rest of the traits had a maximum difference of 3 mm and were considered for analysis. For Individuals B and C no measurements fell outside of 3 mm difference between trials, so all measurements were input into FORDISC initially.

Some measurements were eliminated from analysis due to each individual having their calvarium, or skullcap, removed as illustrated in **Figure 32**. This would have specifically affected the occipital chord measurement. These measurements routinely showed to be outside of three standard deviations and were eliminated from analysis, as exemplified by **Figure 13a**.

To simplify classifications made by the program, measurements outside of two standard deviations were removed from analysis. Also removed were ancestral groups of the opposite sex than that estimated for individuals. For example, Individual C was estimated to be female, so any male ancestral groups were eliminated. After these eliminations, a goal total correct assessment of 65% was met (**Figure 13c**), and FORDISC classified the individual into an ancestral group based on the measurements distance from the mean.

Table 12.

Cranial measurements taken for ancestry assessment with FORDISC 3.1 program. Cranial measurements were measured in millimeters. Measurements were averaged and rounded to the nearest millimeter for FORDISC analysis (mm).

	A		B		C	
Maximum Cranial Length (GOL)	166	165	179	179	166	166
Maximum Cranial Breadth (XCB)	123	123	127	128	121	120
Bizygomatic Breadth (ZYB)	111	110	128	128	109	109
Basion-Bregma Height (BBH)	123	123	125	125	124	124
Cranial Base Length (BNL)	95	95	100	99	95	94
Basion-Prosthion Length (BPL)	95	86	95	95	90	91
Max. Alveolar Breadth (MAB)	56	55	65	66	52	52
Max. Alveolar Length (MAL)	50	49	54	54	50	50
Biauricular Breadth (AUB)	102	101	115	115	100	100
Upper Facial Height (UFHT)	59	57	66	66	62	61
Minimum Frontal Breadth (WFB)	89	89	95	95	86	86
Upper Facial Breadth (UFBR)	97	96	110	109	96	96
Nasal Height (NLH)	46	46	51	51	44	44
Nasal Breadth (NLB)	19	20	28	29	25	24
Orbital Breadth (OBB)	36	35	41	41	37	38
Orbital Height (OBH)	33	33	35	35	33	34
Biorbital Breadth (EKB)	85	87	99	98	89	88
Interorbital Breadth (DKB)	21	21	28	29	21	21
Frontal Chord (FRC)	107	107	110	109	102	102
Parietal Chord (PAC)	100	100	115	113	106	106
Occipital Chord (OCC)	89	89	86	84	81	81
Foramen Magnum Length (FOL)	31	31	35	35	33	33
Foramen Magnum Breadth (FOB)	26	26	30	30	26	25
Mastoid Height (MDH)	20	23	28	29	24	21

a)

Current Case		Chk	Group	Classified into	Distance from
AUB	100	---	BF	**BF**	24.2
BBH	124	--	WF		28.5
BNL	94	-	JF		29.0
BPL	91	-	HF		29.1
FRC	102	-	BM		38.5
GOL	166	-	AF		39.6
MAB	52	--	HM		41.4
NLB	24		GTM		43.3
NLH	44	--	WM		46.3
OBB	38	-	CHM		47.4
OBH	34		VM		48.4
OCC	81	---	JM		52.2
PAC	106	-	AM		59.0
UFHT	61	--			
WFB	86	--			
XCB	120	---			
ZYB	109	---			

b)

Group	Classified into	Distance from
JF	**JF**	0.7
HF		0.8
BF		3.1
WF		4.1

Current Case is closest to JFs

c)

From Group	Total Number	Into Group BF	HF	JF	WF	Correct
BF	80	47	9	18	6	58.8 %
HF	57	8	22	14	13	38.6 %
JF	62	20	16	24	2	38.7 %
WF	257	8	24	13	212	82.5 %

Total Correct: 305 out of 456 (66.9 %) *** CROSS-VALIDATED ***

Fig. 13 An illustration of the FORDISC process for assessing ancestry. **A)** Initial assessment of cranial measurements and sorting into ancestral of Individual C by the FORDISC program. The program assesses each input measurement based on the means of all included ancestral groups. Each – or + indicates the measurement is at least on standard deviation from the mean. The measurements are also classified into the ancestral group that is closest based on standard deviations. Using all measurements, Individual C is initially sorted into the Black Female (BF) group. **B)** Final classification of Individual C based on ancestral groups within FORDISC 3.1. After removal of measurements two standard deviations of more, and removing any male ancestral groups, Individual C was sorted into the Japanese Female (JF) ancestral group. **C)** The probabilities assessed for each ancestral group compared to the final selection of measurements. The correct percentage is an indication of the number of matches between the current case and the number of cases within the lone ancestral group. Important is the total correct matches, which totals all correct matches compared to all cases for the included ancestral groups. A minimum of 65% total correct matches was required for this thesis.

The final estimation of ancestry is reported in **Table 13**. Individual A was estimated as a White Female, with a total correct assessment of 69.2%. Individual B was estimated to be a White Male, with a total correct assessment of 77.4%. Individual C was estimated to be an East Asian Female, with a total correct assessment of 66.9%

Table 13.

Sex and ancestry assignments for FORDISC of the three individuals.

Individual	Sex	Ancestry Assignment	Total Correct
A	F	European (Caucasian)	69.2%
B	M	European (Caucasian)	77.4%
C	F	Japanese (East Asian)	66.9%

3.2 Isolation of DNA

After the biological profile was completed, a molar was extracted from each individual, and at least two attempts to isolate DNA were performed. Quantifiable amounts of DNA were reported in **Table 14** for all attempts. The Qubit Fluorometer has a limit of detection of 0.200 ng of DNA when using the High Sensitivity Assay Kit.

For tooth MT, isolation attempt 2 and 3 were both altered by increasing the incubation temperature to 57 ºC. It was observed that DNA concentrations did increase as temperature increased. Less tooth sample was required to reach the same concentrations.

Table 14.

DNA yield from tooth samples after cleaning. The Qubit 2.0 Fluorometer has a limit of detection (LOD) of 0.200 ng/µL. A concentration lower than the LOD is reported as *<0.200*.

Sample (Extraction Attempt)	Tooth Powder (mg)	DNA Yield (ng/µL)
A (Attempt 1)	201.7	0.571
A (Attempt 2)	329.9	0.993
B (Attempt 1)	200.4	*<0.200*
B (Attempt 2)	257.3	0.520
B (Attempt 3)	177.2	0.830
C (Attempt 1)	208.9	*<0.200*
C (Attempt 2)	192.7	0.318
MT (Attempt 1)	216.22	0.236
MT (Attempt 2)	131.3	0.216
MT (Attempt 3)	74.8	0.208

3.2.1 Sequencing of Mitochondrial DNA

Mitochondrial DNA segments were isolated using the DNA primers listed in **Table 6**. After PCR was performed, a check was performed for each individual using the TapeStation 2200 instrument. Present bands indicated a success, while a lack of bands indicated the run failed. For Individual A, the TapeStation results are shown in **Figure 14**. All runs that were confirmed to be successful were sequenced. **Figure 15** shows a snapshot of the successful sequencing runs for Individual A, for whom large sections of both HVRI and HVRII were isolated.

In HVRI of Individual A, two partial sequences were obtained, and although they did not overlap, there was only a loss of 8 bases (**Figure 16a**). In HVRII, only one sequence was obtained for 191 bases. In this sequence, the genetic analyzer detected some errors, highlighted in yellow in **Figure 15b**. These errors are sizing errors, due to an abnormally large peak masking nearby peaks. These errors were manually overridden by the researcher.

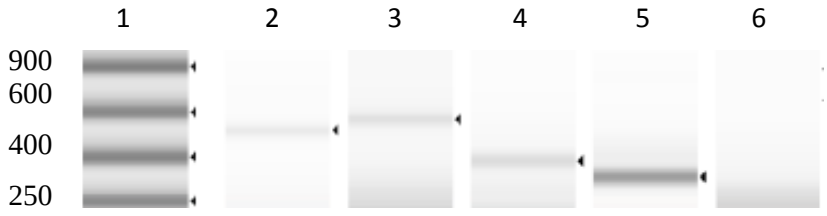

Fig. 14. Yield gel results of Individual A developed by TapeStation electrophoresis. Lanes 2 and 3 represent PCR attempts in HVRI. Lanes 4, 5, and 6 represent HVRII.

a)

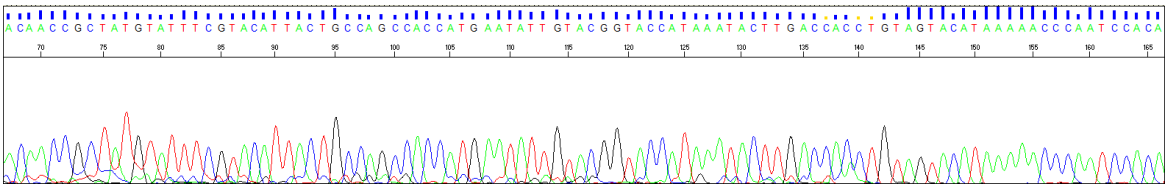

b)

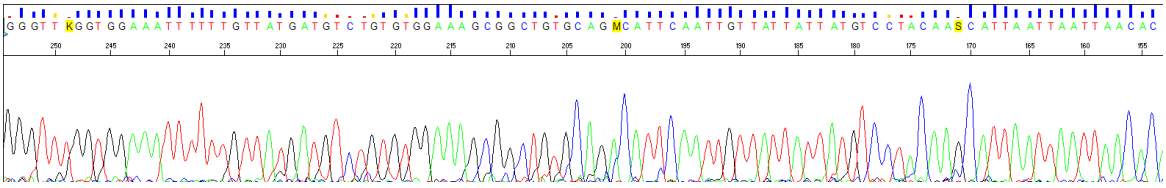

Fig. 15. a) Snapshot of the mtDNA sequence from the HVRI obtained from Individual A. Two partial sequences from this region were able to be extracted. No base pair errors were observed. **b)** Snapshot of the mtDNA sequence from the HVRII obtained from Individual A. One sequence was able to be extracted from the samples. Any errors caused by overlapping peaks are highlighted yellow.

a)

```
Query  1      CCACCCAAGTATTGACTCACCCATCAACAACCGCTATGTATTTCGTACATTACTGCCAGC  60
              ||||||||||||||||||||||||||||||||||||||||||||||||||||||||||||
Sbjct  16052  CCACCCAAGTATTGACTCACCCATCAACAACCGCTATGTATTTCGTACATTACTGCCAGC  16111

Query  61     CACCATGAATATTGTACGGTACCATAAATACTTGACCACCTGTAGTACATAAAAACCCAA  120
              ||||||||||||||||||||||||||||||||||||||||||||||||||||||||||||
Sbjct  16112  CACCATGAATATTGTACGGTACCATAAATACTTGACCACCTGTAGTACATAAAAACCCAA  16171

Query  121    TCCACATCAAAACCCCCTCCCCATGCTTACAAGCAAGTACAGCAATCAACCCTCAACTAT  180
              ||||||||||||||||||||||||||||||||||||||||||||||||||||||||||||
Sbjct  16172  TCCACATCAAAACCCCCTCCCCATGCTTACAAGCAAGTACAGCAATCAACCCTCAACTAT  16231

Query  181    CACACATCAACTGCAACTCCAAAGCCACCCCTCACCCACTAGGATACCAGGATACCAACA  240
              ||||||||||||||||||||||||||||||||||||||||||||||||||||||||||||
Sbjct  16232  CACACATCAACTGCAACTCCAAAGCCACCCCTCACCCACT--------AGGATACCAACA  16283

Query  241    AACCTACCCACCCTTAACAGTACATAGTACATAAAGCCATTTACCGTACATAGCACATTA  300
              ||||||||||||||||||||||||||||||||||||||||||||||||||||||||||||
Sbjct  16284  AACCTACCCACCCTTAACAGTACATAGTACATAAAGCCATTTACCGTACATAGCACATTA  16343

Query  301    CAGTCAAATCCCTTCTCGTCCCCATGGATGACCCCCCTCAGATAGGGGTCCCTTGACCAC  360
              ||||||||||||||||||||||||||||||||||||||||||||||||||||||||||||
Sbjct  16344  CAGTCAAATCCCTTCTCGTCCCCATGGATGACCCCCCTCAGATAGGGGTCCCTTGACCAC  16403

Query  361    CATCCTC  367
              |||||||
Sbjct  16404  CATCCTC  16410
```

b)

```
Query  1    TATGTCGCAGTATCTGTCTTTGATTCCTGCCTCATCCTATTATTTATCGCACCTACGTTC  60
            ||||||||||||||||||||||||||||||||||||||||||||||||||||||||||||
Sbjct  115  TATGTCGCAGTATCTGTCTTTGATTCCTGCCTCATCCTATTATTTATCGCACCTACGTTC  174

Query  61   AATATTACAGGCGAACATACTTACTAAAGTGTGTTAATTAATTAATGCTTGTAGGACATA  120
            ||||||||||||||||||||||||||||||||||||||||||||||||||||||||||||
Sbjct  175  AATATTACAGGCGAACATACTTACTAAAGTGTGTTAATTAATTAATGCTTGTAGGACATA  234

Query  121  ATAATAACAATTGAATGTCTGCACAGCCGCTTTCCACACAGACATCATAACAAAAAATTT  180
            |||||||||||||||||||||||||||||| ||||||||||||||||||||||||||||
Sbjct  235  ATAATAACAATTGAATGTCTGCACAGCCACTTTCCACACAGACATCATAACAAAAAATTT  294

Query  181  CCACCAAACCC  191
            ||||||||||
Sbjct  295  CCACCAAACCC  305
```

Fig. 16. Compiled sequences of all DNA fragments from Individual A compared to the revised Cambridge Reference Sequence. **a.** (Top) Sequence from HVR1 **b.** (Bottom) Sequence from HVRII.

For Individual B, the TapeStation results are shown in **Figure 17**. All runs that were confirmed to be successful were then subjected to sequencing, and snapshots were taken (**Figure 18**)**.** For Individual B, sections of both HVRI and HVRII were isolated, though the faint band for HVRI reported by the TapeStation indicated that the PCR was not sufficient.

In HVRI of Individual B, one partial sequence of 21 bases was obtained (**Figure 19a**). In HVRII, three partial sequences were obtained that when overlapped gave a profile of 165 bases (**Figure 19b**).

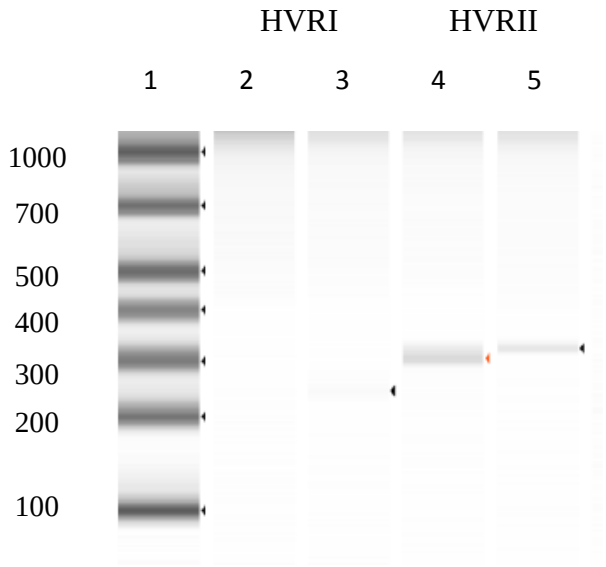

Fig. 17. TapeStation electrophoresis results for Individual B. Lanes 2 and 3 represent PCR attempts in HVRI, which did not replicate well. Lanes 4 and 5 represent HVRII, where stronger bands have appeared.

a)

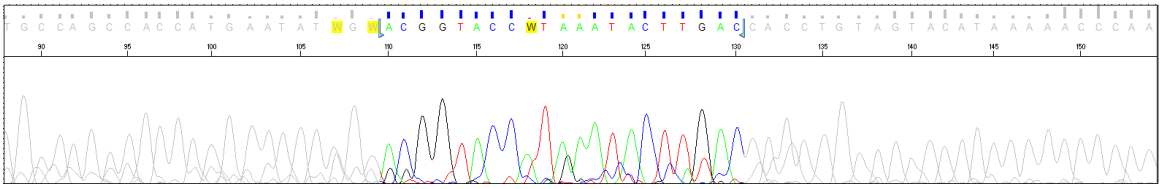

b)

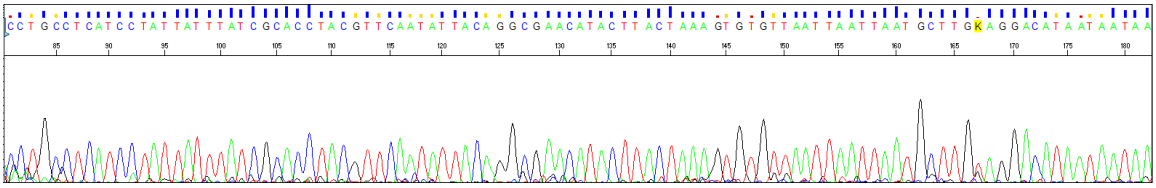

Fig. 18 a) Snapshot of the mtDNA sequence from the HVR1 obtained from Individual B. One partial sequences from this region were able to be extracted. Peaks in gray are failures due to errors in peak height or spacing. These peaks can be manually read, despite these inconstancies. **b)** Snapshot of the mtDNA sequence from the HVRII obtained from Individual B. Three partial sequences from this region were able to be extracted.

a)

```
Query  1      ACGGTACCATAAATACTTGAC  21
              |||||||||||||||||||||
Sbjct  16127  ACGGTACCATAAATACTTGAC  16147
```

b)

```
Query  1    CCTGCCTCATCCTATTATTTATCGCACCTACGTTCAATATTACAGGCGAACATACTTACT  60
            ||||||||||||||||||||||||||||||||||||||||||||||||||||||||||||
Sbjct  140  CCTGCCTCATCCTATTATTTATCGCACCTACGTTCAATATTACAGGCGAACATACTTACT  199

Query  61   AAAGTGTGTTAATTAATTAATGCTTGTAGGACATAATAATAACAATTGAATGTCTGCACA  120
            ||||||||||||||||||||||||||||||||||||||||||||||||||||||||||||
Sbjct  200  AAAGTGTGTTAATTAATTAATGCTTGTAGGACATAATAATAACAATTGAATGTCTGCACA  259

Query  121  GCCGCTTTCCACACAGACATCATAACAAAAAATTTCCACCAAACC  165
            ||| ||||||||||||||||||||||||||||||||||||||||
Sbjct  260  GCCACTTTCCACACAGACATCATAACAAAAAATTTCCACCAAACC  304
```

Fig. 19. Compiled sequences of all DNA fragments from Individual B compared to the revised Cambridge Reference Sequence. **a.** (Left) Sequence from HVR1 **b.** (Right) Sequence from HVRII.

For Individual C, the TapeStation results are shown in **Figure 20**. All runs that were confirmed to be successful were sequenced, and snapshots were taken (**Figure 21**)**.** For Individual C, only HVRI was successfully isolated. In HVRI of Individual C, a complete sequence of 434 bases was obtained (**Figure 22**).

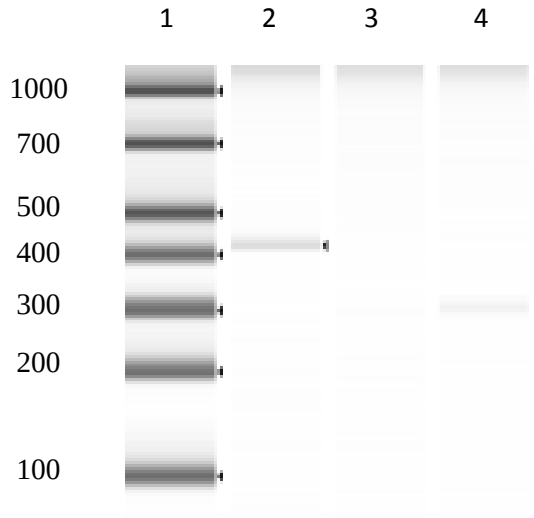

Fig. 20. TapeStation electrophoresis results for Individual C. Lanes 2, 3 and 4 represent PCR attempts in HVRI, for which lanes 3 and 4 did not replicate well, though a faint band in lane 4 indicates a 300 base pair product did partially form.

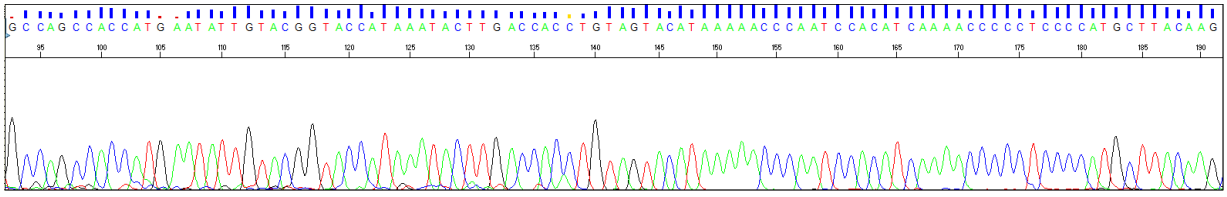

Fig. 21. Snapshot of the mtDNA sequence from the HVR1 obtained from Individual C. Two partial sequences from this region were able to be extracted.

```
Query  2      CACCATTAGCACCCAAAGCTAAGATTCTAATTTAAACTATTCTCTGTTCTTTCATGGGGA  61
              ||||||||||||||||||||||||||||||||||||||||||||||||||||||||||||
Sbjct  15978  CACCATTAGCACCCAAAGCTAAGATTCTAATTTAAACTATTCTCTGTTCTTTCATGGGGA  16037

Query  62     AGCAGATTTGGGTACCACCCAAGTATTGACTCACCCATCAACAACCGCTATGTATTTCGT  121
              ||||||||||||||||||||||||||||||||||||||||||||||||||||||||||||
Sbjct  16038  AGCAGATTTGGGTACCACCCAAGTATTGACTCACCCATCAACAACCGCTATGTATTTCGT  16097

Query  122    ACATTACTGCCAGCCACCATGAATATTGTACGGTACCATAAATACTTGACCACCTGTAGT  181
              ||||||||||||||||||||||||||||||||||||||||||||||||||||||||||||
Sbjct  16098  ACATTACTGCCAGCCACCATGAATATTGTACGGTACCATAAATACTTGACCACCTGTAGT  16157

Query  182    ACATAAAAACCCAATCCACATCAAAACCCCCTCCCCATGCTTACAAGCAAGTACAGCAAT  241
              ||||||||||||||||||||||||||||||||||||||||||||||||||||||||||||
Sbjct  16158  ACATAAAAACCCAATCCACATCAAAACCCCCTCCCCATGCTTACAAGCAAGTACAGCAAT  16217

Query  242    CAACCCTCAACTATCACACATCAACTGCAACTCCAAAGCCACCCCTCACCCACTAGGATA  301
              ||||||||||||||||||||||||||||||||||||||||||||||||||||||||||||
Sbjct  16218  CAACCCTCAACTATCACACATCAACTGCAACTCCAAAGCCACCCCTCACCCACTAGGATA  16277

Query  302    CCAACAAACCTACCCACCCTTAACAGTACATAGTACATAAAGCCATTTACCGTACATAGC  361
              ||||||||||||||||||||||||||||||||||||||||||||||||||||||||||||
Sbjct  16278  CCAACAAACCTACCCACCCTTAACAGTACATAGTACATAAAGCCATTTACCGTACATAGC  16337

Query  362    ACATTACAGTCAAATCCCTTCTCGTCCCCATGGATGACCCCCCTCAGATAGGGGTCCCTT  421
              ||||||||||||||||||||||||||||||||||||||||||||||||||||||||||||
Sbjct  16338  ACATTACAGTCAAATCCCTTCTCGTCCCCATGGATGACCCCCCTCAGATAGGGGTCCCTT  16397

Query  422    GACCACCATCCTC  434
              |||||||||||||
Sbjct  16398  GACCACCATCCTC  16410
```

Fig. 22. Compiled sequences of all DNA fragments from Individual C compared to the revised Cambridge Reference Sequence. Sequence from HVR1.

For tooth MT, the TapeStation results are shown in **Figure 23**. For lanes 2, 5, 7, and 8 too much DNA sample was used for PCR, resulting in the large dark bands. All runs that were confirmed to be successful were sequenced, and snapshots were taken (**Figure 24**)**.** For tooth MT, complete sequences were isolated for HVRI and HVRII.

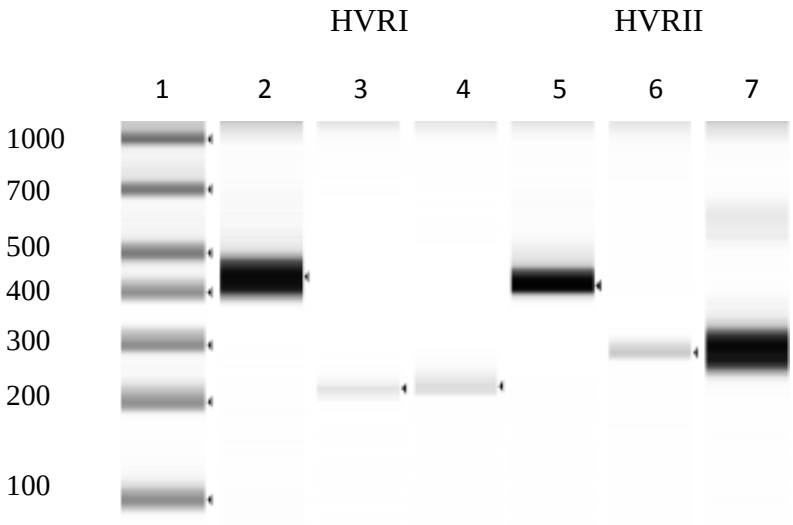

Fig. 23. TapeStation electrophoresis results for tooth sample MT. Lanes 2, 3 and 4 represent PCR attempts in HVRI. Lane 2 replicated the whole region, while Lanes 3 and 4 were each contain overlapping half sequences. Lanes 5, 6, 7 and 8 represent HVRII. Lane 5 represents the whole region, Lanes 6 and 7 are half sequences.

a)

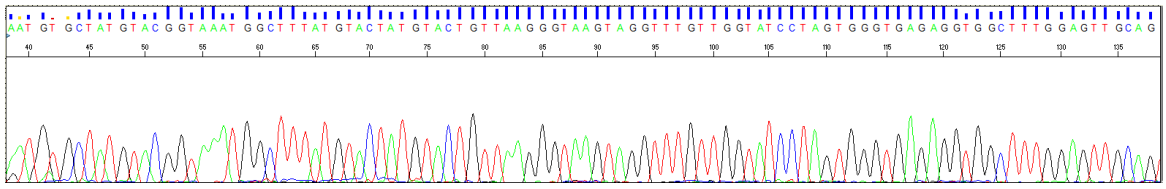

b)

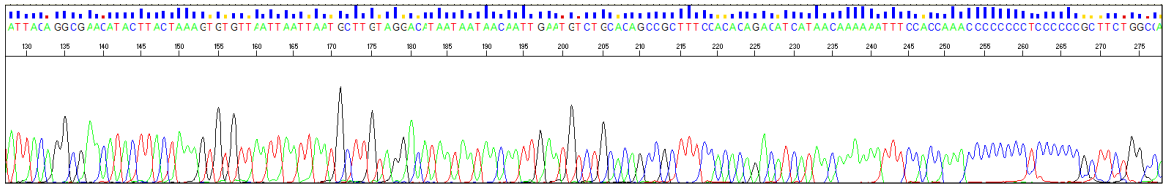

Fig. 24. a) Snapshot of the mtDNA sequence from the HVR1 obtained from tooth MT. Three partial sequences from this region were able to be extracted. **b)** Snapshot of the mtDNA sequence from the HVRII obtained from tooth MT. Three partial sequences from this region were able to be extracted.

a)

```
Query  2      CACCATTAGCACCCAAAGCTAAGATTCTAATTTAAACTATTCTCTGTTCTTTCATGGGGA  61
              ||||||||||||||||||||||||||||||||||||||||||||||||||||||||||||
Sbjct  15978  CACCATTAGCACCCAAAGCTAAGATTCTAATTTAAACTATTCTCTGTTCTTTCATGGGGA  16037

Query  62     AGCAGATTTGGGTACCACCCAAGTATTGACTCACCCATCAACAACCGCTATGTATTTCGT  121
              ||||||||||||||||||||||||||||||||||||||||||||||||||||||||||||
Sbjct  16038  AGCAGATTTGGGTACCACCCAAGTATTGACTCACCCATCAACAACCGCTATGTATTTCGT  16097

Query  122    ACATTACTGCCAGCCACCATGAATATTGTACGGTACCATAAATACTTGACCACCTGTAGT  181
              ||||||||||||||||||||||||||||||||||||||||||||||||||||||||||||
Sbjct  16098  ACATTACTGCCAGCCACCATGAATATTGTACGGTACCATAAATACTTGACCACCTGTAGT  16157

Query  182    ACATAAAAACCCAATCCACATCAAAACCCCCTCCCCATGCTTACAAGCAAGTACAGCAAT  241
              ||||||||||||||||||||||||||||||||||||||||||||||||||||||||||||
Sbjct  16158  ACATAAAAACCCAATCCACATCAAAACCCCCTCCCCATGCTTACAAGCAAGTACAGCAAT  16217

Query  242    CAACCCTCAACTATCACGCATCAACTGCAACTCCAAAGCCACCCTCTCACCCACTAGGATA  301
              ||||||||||||||||||||||||||||||||||||||||||||||||||||||||||||
Sbjct  16218  CAACCCTCAACTATCACACATCAACTGCAACTCCAAAGCCACCCCTCACCCACTAGGATA  16277

Query  302    CCAACAAACCTACTTACCCTTAACAGTACATAGTACATAAAGCCATTTACCGTACATAGC  361
              ||||||||||| ||||||||||||||||||||||||||||||||||||||||||||||||
Sbjct  16278  CCAACAAACCTACCCACCCTTAACAGTACATAGTACATAAAGCCATTTACCGTACATAGC  16337

Query  362    ACATTACAGTCAAATCCCTTCTCGTCCCCATGGATGACCCCCCTCAGATAGGGGTCCCTT  421
              ||||||||||||||||||||||||||||||||||||||||||||||||||||||||||||
Sbjct  16338  ACATTACAGTCAAATCCCTTCTCGTCCCCATGGATGACCCCCCTCAGATAGGGGTCCCTT  16397

Query  422    GACCACCATCCTC  434
              |||||||||||||
Sbjct  16398  GACCACCATCCTC  16410
```

b)

```
Query  1      GCCGGAGCACCCTATGTCGCAGTATCTGTCTTTGATTCCTGCCTCATCCCATTATTTATC  60
              ||||||||||||||||||||||||||||||||||||||||||||||||||||||||||||
Sbjct  103    GCCGGAGCACCCTATGTCGCAGTATCTGTCTTTGATTCCTGCCTCATCCTATTATTTATC  162

Query  61     GCACCTACGTTCAATATTACAGGCGAACATACTTACTAAAGTGTGTTAATTAATTAATGC  120
              ||||||||||||||||||||||||||||||||||||||||||||||||||||||||||||
Sbjct  163    GCACCTACGTTCAATATTACAGGCGAACATACTTACTAAAGTGTGTTAATTAATTAATGC  222

Query  121    TTGTAGGACATAATAATAACAATTGAATGTCTGCACAGCCGCTTTCCACACAGACATCAT  180
              ||||||||||||||||||||||||||||||||||||||||||||||||||||||||||||
Sbjct  223    TTGTAGGACATAATAATAACAATTGAATGTCTGCACAGCCACTTTCCACACAGACATCAT  282

Query  181    AACAAAAAAATTTCCACCAAAccccccccctcccccGCTTCTGGCCACAGCACTTAAACAC  240
              |||||||||||||||||||||||||| | ||||||||||||||||||||||||||||||
Sbjct  283    AACAAAAAAATTTCCACCAAACCCCCCC-T-CCCCCGCTTCTGGCCACAGCACTTAAACAC  340

Query  241    ATCTCTGCCAAACCCCAAAAACAAAGAACCCTAACACC  278
              |||||||||||||||||||||||||||||||||||||
Sbjct  341    ATCTCTGCCAAACCCCAAAAACAAAGAACCCTAACACC  378
```

Fig. 25. Compiled sequences of all DNA fragments from tooth MT compared to the revised Cambridge Reference Sequence. **a.** (Top) Sequence from HVR1 **b.** (Bottom) Sequence from HVRII.

For reference, the sequence of researcher JS was obtained from both HVRI and HVRII (**Figure 26**). All sequences were compared to the rCRS, and SNPs were recorded in **Table 15**. Tooth MT had the most SNPs with a total of 8 and was the only sample to record SNPs in HVRI. Based on the sequences that were obtained, Individual A and B both reported one SNP in HVRII, which was also reported by researcher JS and tooth MT (**Table 16**). Of the observed SNPs, the adenine to guanine change from the rCRS at base 263 was the most common.

Based on the available SNPs, each individual was assessed as Haplogroup H2. Haplogroup H2 is most commonly associated with areas of Eastern Europe, including the Caucasuses, though it may have originated in Western Europe (60).

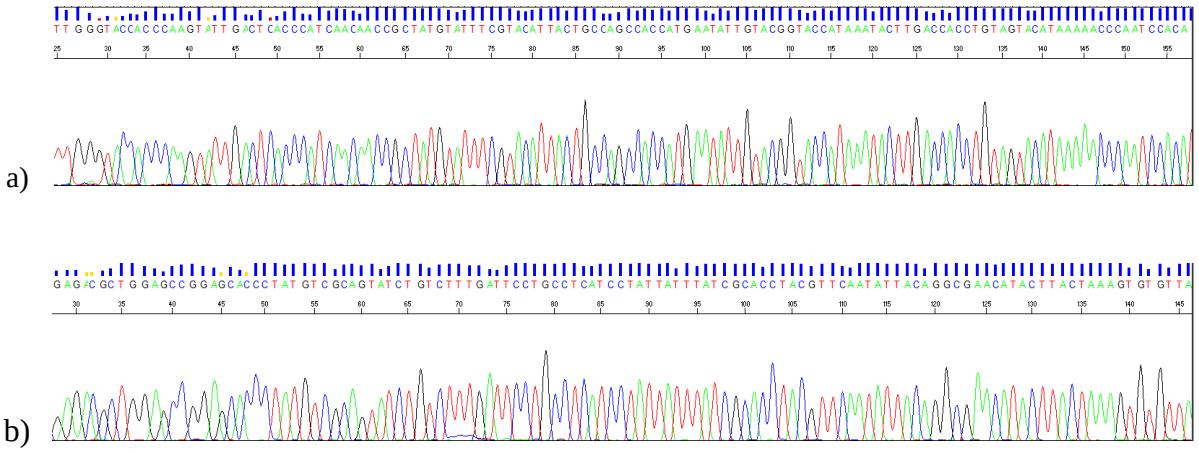

Fig. 26. a) Snapshot of the mtDNA sequence from the HVR1 obtained from researcher JS **b)** Snapshot of the mtDNA sequence from the HVRII obtained from researcher JS.

Table 15.

Full list of SNPs for each individual, and the assigned haplogroups based on the mutations in the mtDNA sequence compared to the rCRS.

Individual	Mutations	Top Match to PhyloTree in HVR1	Top Match to PhyloTree in HVRII	Overall Haplogroup
A	263G	H2a2a1	H2a2a	H2
B	263G	NA	H2a2a	H2
C	NA	H2a2a1	NA	H2
MT	16235G 16261T 16291T 16292T 152C, 263G, (309.1C), (315.1C)	H2a2b1	H2a2a2	H2
JS	263G (309.1C) (315.1C)	H2a2a1	H2a2a	H2

Table 16.

Total occurrence of observed SNPs. The lower the occurrence, the rarer the SNP is. Frequency data is derived from 42616 GenBank sequences and 69557 Control Region sequences (www.mitomap.org).

Mutation	Occurrence	Individuals
16235G	817	MT
16261T	7589	MT
16291T	3102	MT
16292T	2619	MT
152C	22857	MT
263G	78186	A, B, MT, JS
(309.1C)	1258	MT, JS
(315.1C)	26712	MT, JS

3.2.2 Analysis of STR Profiles

An STR profile was attempted to determine if nuclear DNA was present and determine sex. Of the five attempts performed on the DNA isolate from Individual A, two resulted in peaks. **Figure 27** is an example of one of the electropherograms with readable peaks. Multiple alleles were recorded at several loci, indicating multiple sources of DNA. The most severe was a reading of locus D3S1358, which reported 11 readable peaks. This indicates a minimum of six possible contributors to this DNA.

A similar observation was made for Individual B. Of the three attempts performed, one resulted in readable peaks. This trial reported one locus that had three alleles (**Table 18**). This indicates a minimum number of 2 contributors for this locus. Only allele 14 can be contributed to researcher JS, but the second allele reported in the profile of researcher JS, allele 12, was not present.

Tooth MT reported a unique profile, for which no more than two peaks appeared in any given locus, shown in **Figure 29**. This indicates that there was no contamination in the DNA isolated from tooth MT, and that there was a high DNA concentration.

Table 17.

Attempts of STR profiles for each individual. If an electropherogram had one peak read by the program, then it was considered to have readable peaks.

Individual	# of Attempts	Samples with Readable Peaks
A	5	2
B	3	1
C	5	0

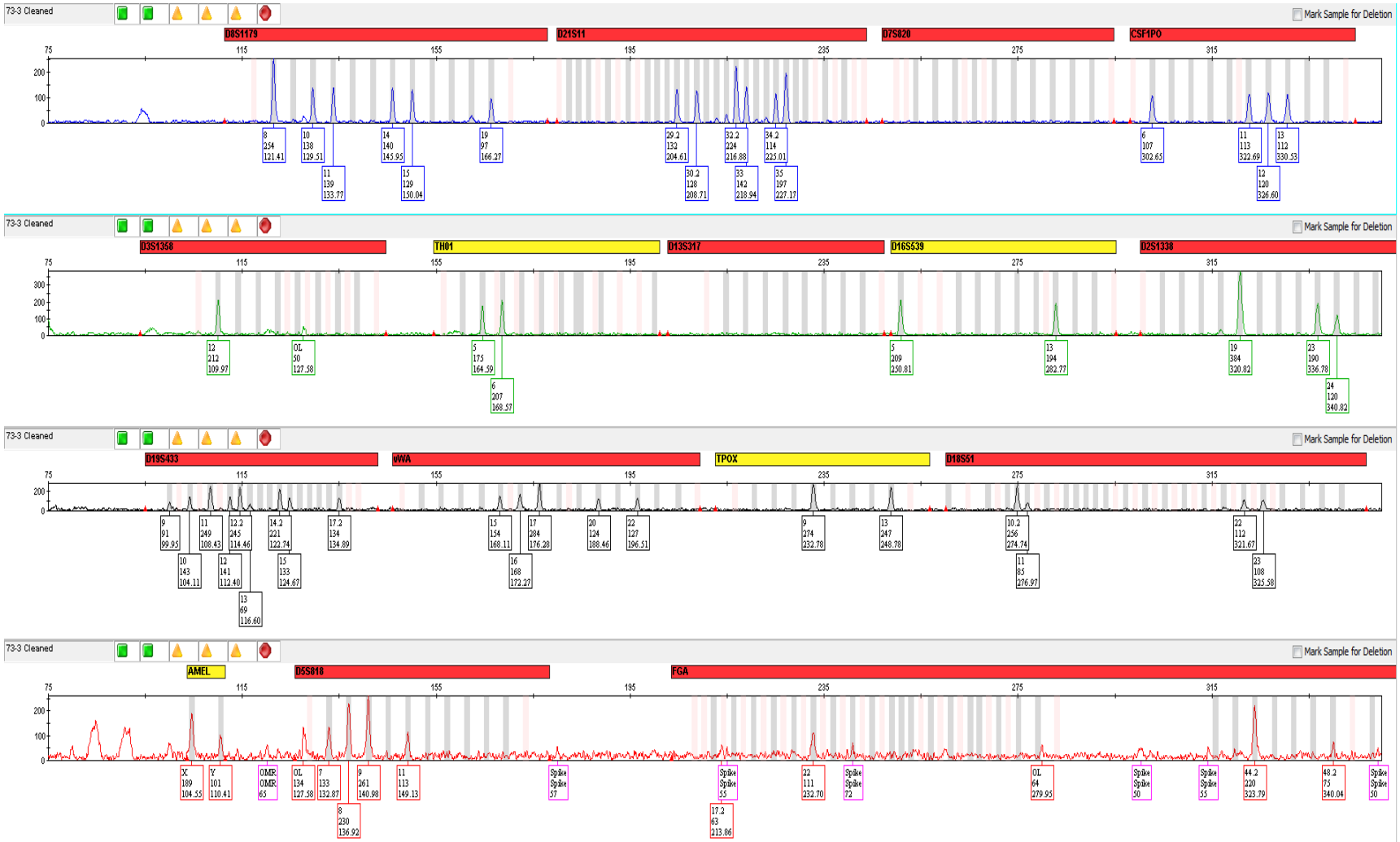

Fig. 27. STR electropherogram of Individual A. Multiple loci show many peaks. In this electropherogram, D19S433 shows ten peaks, indicating a minimum of five contributors.

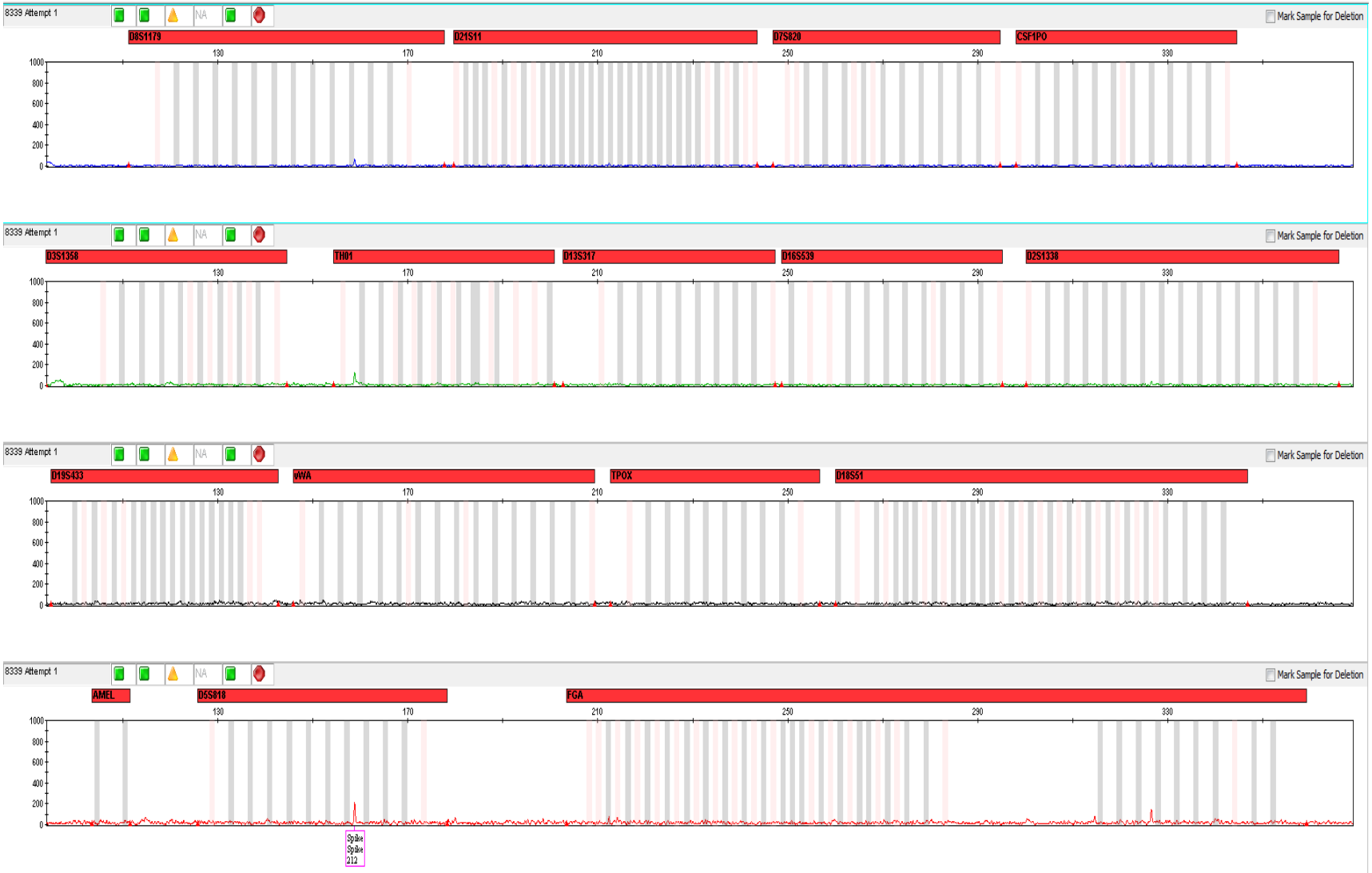

Fig. 28. STR electropherogram of Individual C. No peaks are present.

Table 18.

List of alleles observed through all STR profile attempts. Individual A had two electropherograms that recorded more than 2 peaks at a locus. Locus D21S11 recorded the most peaks in one reading at 11, which indicates that a minimum of 6 individuals had to contribute DNA. Italicized numbers represent peaks with RFU values less than 200.

	JS	Individual A	Individual B	Individual C	Tooth MT
D8S1179	12, 14	*8*, *9*, *10*, 11, 12, 13, 14, *18*	10, *14*, *15*	N/A	14
D21S11	30, 32.2	27, 28, *28.2*, *29*, *29.2*, 30, *31*, *31.2*, *32*, *32.2*, 33.2	*OL(27.2)*, 32	N/A	30, 31.2
D7S820	10, 11	6, *7*, *9*, *10*, *11*	N/A	N/A	9, 11
CSF1PO	12	*12*	N/A	N/A	11
D3S1358	14, 18	12, *13*, 14, *15*, 16, 17, 18, 19	14, 18	N/A	16
TH01	6, 9.3	6, 8, 9.3, *11*	6, *9.3*	N/A	6, 9.3
D13S317	11, 12	10, 11, 13	N/A	N/A	12, 14
D16S539	11	9, 10, 11	N/A	N/A	12, 13
D2S1338	19, 24	*16*, *19*	19, 25	N/A	20, 25
D19S433	14, 15.2	*9*, *10*, *10.2*, 12, *13*, *13.2*, 14, 14.2, *15* 15.2, *17.2*	N/A	N/A	15
vWA	16, 17	*13*, 16, 17, 18	N/A	N/A	17, 18
TPOX	8, 9	*6*, *7*, 8, *10*, 12	N/A	N/A	8
D18S51	15, 16	*9*, *15*, *16*	N/A	N/A	14, 15
Amelogenin	X, Y	X, Y	X, *Y*	N/A	X
D5S818	11, 12	*8*, *9*, 10, 11, 12, *13*, *14*, *15*, *16*, *17*	N/A	N/A	12, 13
FGA	22, 25	17, *17.2*, *18*, *19*, 22, *24*, *25*, *28*, *29*, *30.2*, *31.2*, *48.2*	N/A	N/A	21, 22

Fig. 29. STR electropherogram of DNA samples from tooth MT. No more than two peaks are present at any given locus.

3.2.3 Y-STR Analysis

Since it was confirmed that researcher JS had a Y-chromosome (**Table 18**), an assessment of paternal ancestry was performed to show how the process would have been performed on the individuals focused on in this study. A Y-STR profile was generated (**Figure 30**), and for each locus, only one allele is expected to be present, other that locus DYS385, which is derived from tandemly duplicated segments of the Y chromosome, thus giving rise to two fragments of variable length (61). The total list of observed Y-STR alleles (**Table 19**) was applied to the Y-Chromosome Haplotype Reference Database (YHRD) for analysis.

For the reported Y-STR profile of researched JS, a total of 12 matches were made out of 145,816 total profiles, or approximately one match in every 12,151 profiles. Of the twelve matches, shown in **Figures 31a**, three quarters of them report to the British Isles. Six profiles reported from Ireland, while the other three matches reported to the United Kingdom. Based on known genealogical information, paternal lineage can be traced back to Ireland.

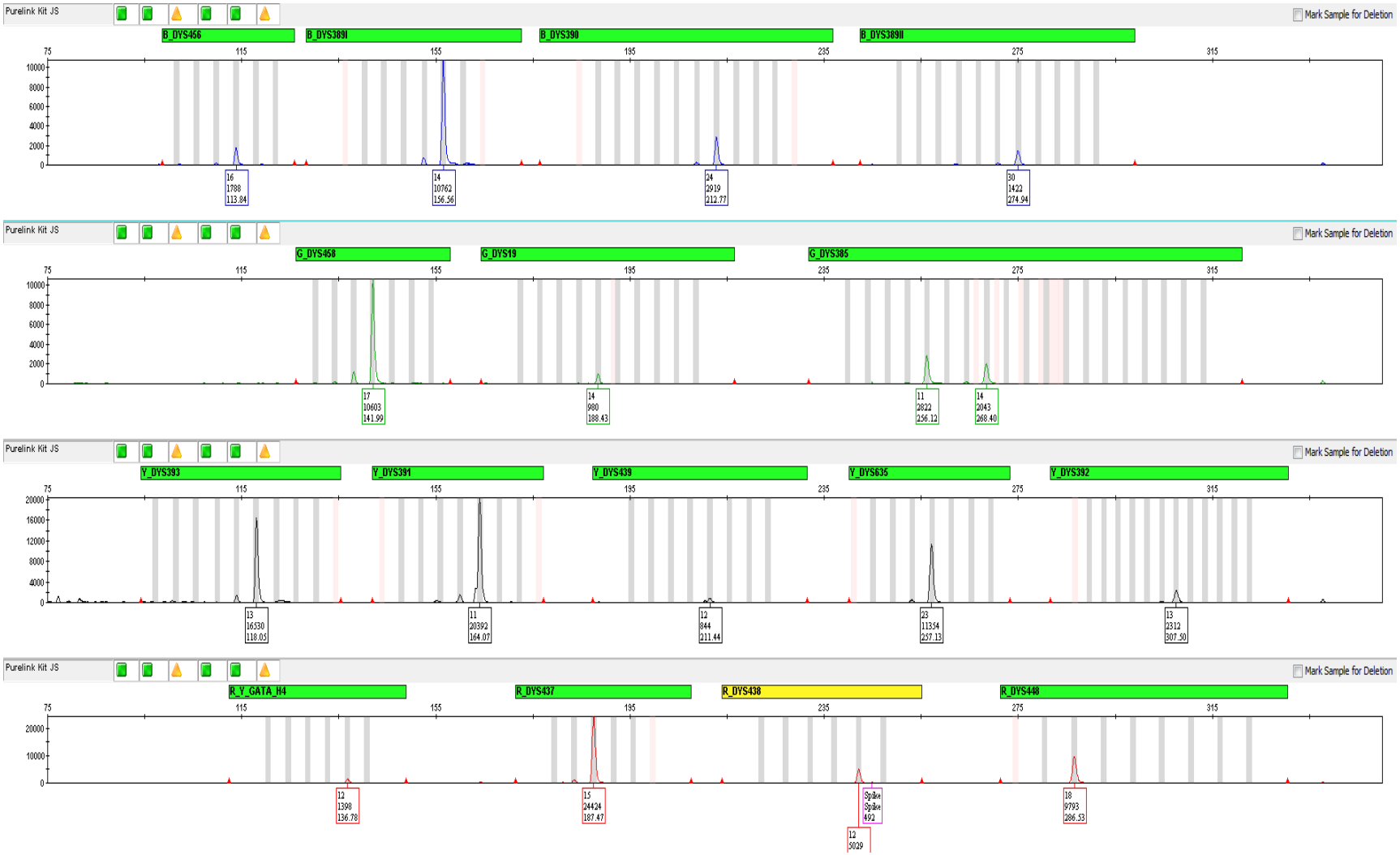

Fig. 30. Y-STR electropherogram of researcher JS.

Table 19.

List of Y-STR alleles observed from JS.

DYS456	16
DYS3891	14
DYS390	24
DYS38911	30
DYS458	17
DYS19	14
DYS385	11, 14
DYS393	13
DYS391	11
DYS439	12
DYS635	23
DYS392	13
YGATAH4	12
DYS437	15
DYS438	12
DYS448	18

a)

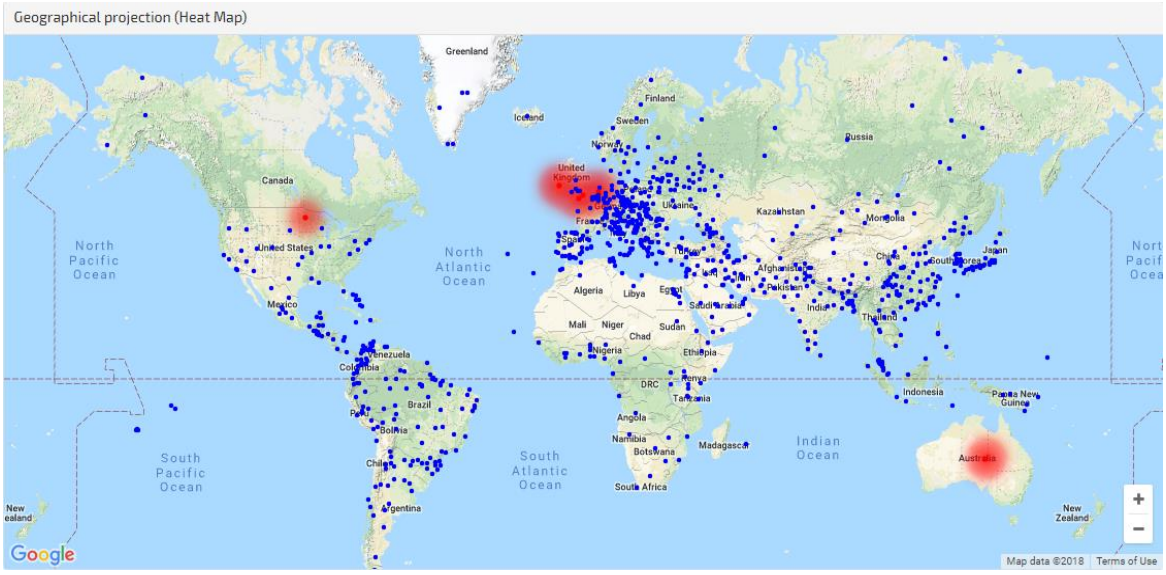

b)

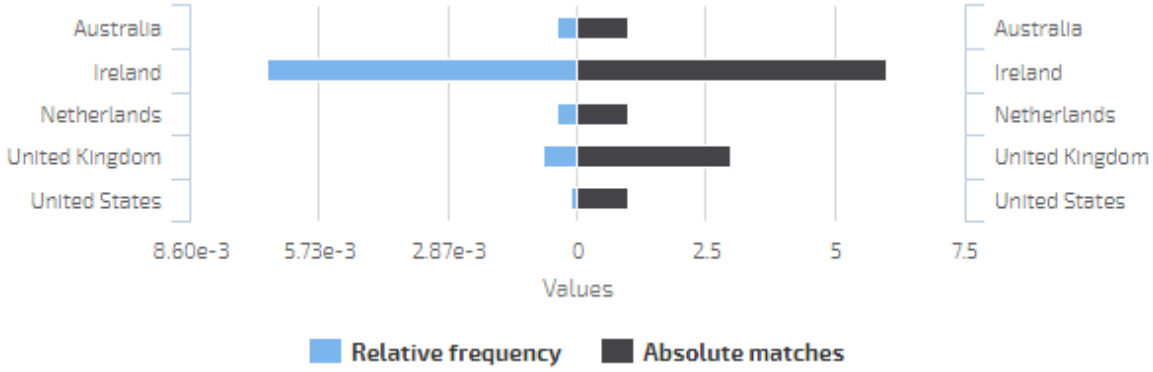

Fig. 31 Results obtained from YHRD **a)** Geographic population analysis of researcher JS. **b)** Ancestry matches based on Y-STR haplotype.

IV. Discussion

4.1 Individual A: 730205-3

For Individual A, the estimations of age and stature are confident because observations and estimations were consistent for both the Suchey-Brooks and Lovejoy methods, and the measurements of the long bones were consistent through both trials. For the estimation of sex and ancestry, some discrepancies were observed.

When assessing sex using the Phenice method, Individual A was estimated to be probable male. The estimation of sex using Buikstra and Ubelaker's cranial traits resulted in the assessment of probable female, although with the Nuchal Crest and the Supra-Orbital Margin each receiving a score of 3 once, these traits are arguably ambiguous. Using the current techniques for estimation of sex, Individual A could be classified as ambiguous. Due to the narrow scale of this research, a definite assessment of sex for Individual A cannot be made. To broaden this research, other pubic traits could be used to estimate sex, such as subpubic concavity angle, pelvic inlet shape, and sciatic notch shape and size (6).

When estimating ancestry, some measurements had to be eliminated from analysis due to postmortem alterations and measurement inconsistencies as previously mentioned in the methods. The final estimation was that Individual A was a European Female.

A nearly complete sequence of both variable regions of the control region of mitochondrial DNA was obtained for Individual A. HVRII stopped short of the C-stretch, a sequence of cytosines running from position 303 through 315. This area commonly exhibits SNPs, which was observed for researcher JS. Successful sequencing of this region could have proved if these samples were contaminated.

The sequences did show an occasional error, mostly attributed to peaks overlapping and the appearance of strong cytosine peaks masking smaller neighbor peaks. When compared to the PhyloTree program, the haplogroup of H2 was assessed for Individual A. Haplogroup H2 is most commonly associated with areas of Eastern Europe. This aligns with the estimated ancestry of White Female assessed by FORDISC.

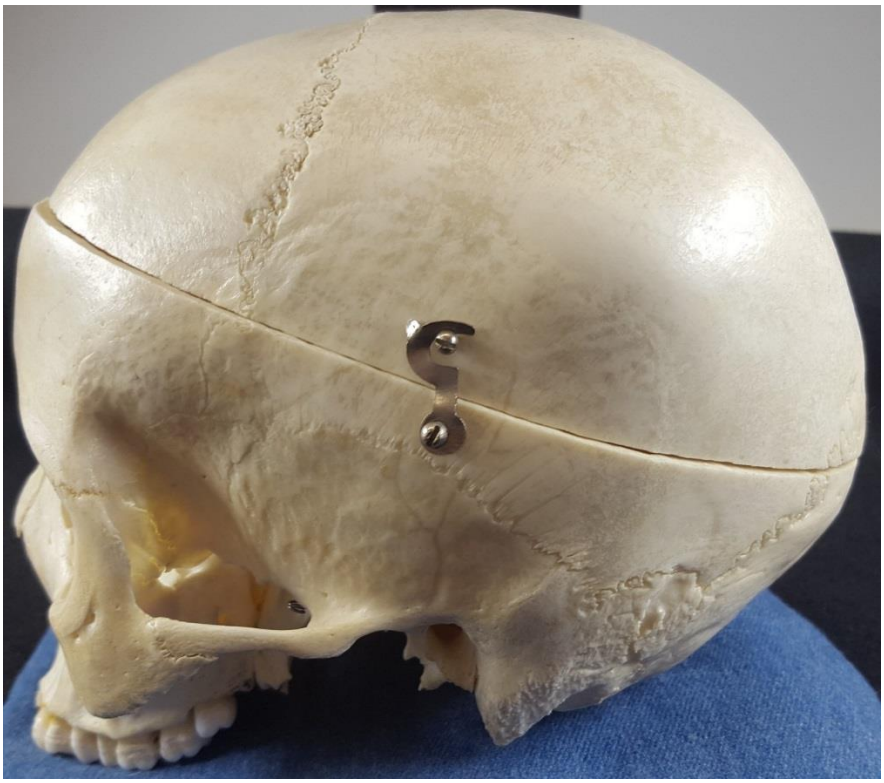

Fig. 32. Side profile of the cranium of Individual C. The cut to allow the removal of the calvarium can be observed.

The final step was to attempt an STR profile to determine sex. Of the five attempts, two resulted in readable peaks. Multiple alleles were recorded at several loci, indicating multiple sources of DNA. This appears to confirm that the samples were contaminated. The most severe was a reading of locus D3S1358, which reported 11 readable peaks. This indicates a minimum of six possible contributors to this DNA. All observed peaks from the STR profile were below 400 RFUs. These low RFU values, combined with the three other runs that all had no recorded peaks, indicates that the tooth samples had no nuclear DNA available for analysis, and that the two runs that did report peaks were contaminated. Thus, any attempts to draw conclusions about sex from the Amelogenin results is confounded by the presence of multiple individuals, making the most likely analytical outcome for Amelogenin to be X,Y.

.

4.2 Individual B:730205-6

For Individual B, the estimations of sex and stature were consistent for both the Phenice pubic and the Buikstra/Ubelaker cranial methods. Additionally, the measurements of the long bones were consistent through both trials. It was for the estimations of age and ancestry that some discrepancies were observed.

When assessing age, the Suchey-Brooks method of analyzing the pubic symphysis was consistent between both trials. Based on the recorded observations, a mean age of 35 was determined. It was in the Lovejoy method that data discrepancies appeared. The two trials performed resulted in different phases reported, with Trial 1 reporting Phase 4 for a minimum age of 35, while Trial 2 reported Phase 5 for a minimum age of 40. Compiling the two methods together, a minimum age of 30 years can be reliably estimated.

When estimating ancestry, again some measurements had to be eliminated from analysis due to each individual having their calvarium removed. Otherwise, no measurements fell outside of 3 mm of difference between trials for Individual B, so all measurements were used for analysis by FORDISC. The final estimation was that Individual B was a European Male.

A nearly complete sequence for HVRII regions was obtained for Individual B, while only one 21-base segment was obtained for HVRI. The HVRII sequence again stopped short of the C-stretch. Without this sequence, it cannot be conclusively proven that samples were contaminated by JS. The sequences did show an occasional error, mostly attributed to peaks overlapping. When compared to the PhyloTree program, the haplogroup of H2 was assessed

for Individual B. This aligns with the estimation of ancestry of a White Male obtained using FORDISC.

Finally, an STR profile was attempted to determine sex. Of the three attempts, only one resulted in peaks. As was observed in the attempts for Individual A, the successful attempt for Individual B resulted in multiple alleles at loci D8S1179 and D21S11, indicating multiple sources of DNA. In this case, the most recorded was three alleles at locus D8S1179. Also, as with Individual A, all observed peaks were below 400 RFUs. These low RFU values, combined with the three other runs that all had no recorded peaks, indicates that the tooth samples had almost no nuclear DNA available for analysis.

4.3 Individual C: 8339

For Individual C, the estimations of sex and age are confident. Observations and estimations were consistent for both the Phenice pubic and the Buikstra/Ubelaker cranial methods, along with the observations recorded for the Phenice and Lovejoy techniques. For Individual C, the estimated age had a mean of 30 years, making this individual younger than the other two. For the estimation of stature and ancestry that some discrepancies were observed.

For the estimation of stature, two sets of equations were required because of the limitations of the selected method. The East Asian Males equations resulted in a smaller possible range, which completely fell within the range created using the White Female equation set.

When estimating ancestry, the final estimation was that Individual C was a Japanese Female, with a total correct assessment of 66.9%. This is the only variant result for ancestral estimation using FORDISC, as the other two individuals were estimated as European individuals. Comparing the recorded cranial measurements, those with the biggest difference when compared to Individuals A and B include the Nasal Breadth, Basion-Prosthion Length, and the Frontal Chord. Most prominent is the Nasal Breadth, which is closer in measurement to the measurements of Individual B, estimated as a male, than when compared to Individual A, estimated as a female.

A nearly complete sequence for the HVRI was obtained for Individual C, however no sequences were obtained for HVRII. No mutations were observed in HVRI, which was also observed in the sequence obtained from researcher JS. When compared to the PhyloTree

program, the haplogroup of H2 was assessed for Individual C. Since Haplogroup H2 is associated with Eastern Europe and the Caucasus mountains, this does not match with the ancestry estimation obtained using FORDISC. An alignment between FORDISC and DNA commonly occurs, but a difference between the estimations can occur due to FORDISC relying on physical traits. This research indicates that Individual C had a maternal lineage that is European in descent.

Finally, an STR profile was attempted to determine sex. Of the three attempts, none of the profiles resulted in peaks at Amelogenin, the sex marker for STR analysis. This indicates that there was no nuclear DNA available for analysis, along with indicating that there was no contaminant DNA that was detected by the genetic analyzer.

4.4 Summation of Observations from Individual A, B, and C

An estimation of ancestry, sex, age, and stature was successfully obtained for each individual. However, some inconsistencies did appear throughout the experiment. For Individual A, the estimation of sex was ambiguous because one method resulted in an assessment of male, the other female. An increase in scope by using further methods could remedy these inconsistencies. The estimation of age could also have been extended. For example, another popular method for estimating age-at-death is through the use of the sternal rib end (2). The methods selected were chosen due to what skeletal material was available, forcing a somewhat limited scope.

It was also apparent that the DNA analysis was limited. The analysis of nuclear DNA through STR profiling repeatedly showed that there was no nuclear DNA present. Any locus that had readable peaks had to be taken into scrutiny because in these cases the majority of loci had a large number of allele peaks, indicating DNA contamination. These readable peaks all had very low RFU values, which occurred because the lower limit of the genetic analyzer was dropped. This was done with the expectation that there would be trace amounts of available DNA.

For each individual, mitochondrial DNA sequences were obtained. The majority of these sequences were highly fragmentary and had to be overlapped in order to develop a full sequence. Because of this, a complete sequence of HVRI and HVRII were not obtained for any of the Individuals A, B, or C, so the possibility that all mutations were not detected exists.

All sequences were compared to the rCRS for SNPs. Most sites use the rCRS as the reference for comparison when assessing ancestry. The purpose of having a mitochondrial DNA reference sequence is to communicate the variation of a lineage in a compact form by listing only the variants of a new lineage relative to the selected reference sequence. The original reference sequence was taken from a European woman in the 1970's (35). A sequence with no deviations from the rCRS, which repeatedly occurred within HVRI, would indicate that the individuals would be from Haplogroup H.

Among the mtDNA haplogroups of Europe, Haplogroup H displays two unique features: an extremely wide geographic distribution and a very high frequency in most of its range. It is by far the most prevalent haplogroup in most European populations, is very common in North Africa and the Middle East, and retains frequencies of 5%–10% even in northern India and Central Asia, at the edges of its distribution range (62).

Another issue with the mtDNA sequences is that they are identical to the sequence developed from the DNA isolate taken from researcher JS. It was expected that there would be at least one mutational difference within the variable regions between two different individuals. This is further an indication that DNA contamination may have occurred.

4.5 Issues with DNA Isolation and Contamination

One of the confirmatory tests run was the use of the Qubit 2.0 Fluorometer to determine the approximate concentration of nuclear DNA obtained from each DNA isolation attempt. The Qubit does not differentiate between human and nonhuman double stranded DNA. This could result in an inflated final concentration reading.

Another issue observed occurred when isolating DNA from tooth MT. Although no increase in concentration was observed when using the Qubit fluorometer, the electropherograms developed using the TapeStation show that there was a lot more DNA isolated from tooth MT than the other tooth samples. This indicates that the Qubit was not detecting the available DNA, bringing into question the isolated DNA from the skeletal material, along with the incubation temperature test conducted using sample from tooth MT.

To combat the risk of DNA contamination, all extracted teeth and any equipment were cleaned. The teeth were cleaned using an absolute ethanol/detergent mixture. This differs from most procedures, which use a 70% ethanol/detergent mixture for cleaning purposes. The increased water dissolves more of the detergent powder to use for cleaning, and also aids in the removal of protein contaminants. Absolute ethanol coagulates proteins, reducing the effectiveness of the wash. This change in the method could have allowed for some contaminant DNA to remain, or protein interference to have occurred.

Negative controls were run throughout the experiment to assess for possible DNA contamination. All controls reported negative results except for one run. When this failure occurred, all solutions and samples that had been run with the negative control were

discarded, remade, and were run again. The next run reported all controls as negative, and the experiment continued as protocols dictated.

As was previously discussed, the results indicate the possibility of DNA contamination. The sequencing results for all three individuals are identical to the sequence obtained for researcher JS. In a typical sequence of non-relatives, there should be some differences. This suggests that the DNA that was sequenced from the three individuals could have been from researcher JS. However, the incomplete, fragmented nature of the sequences leaves open the possibility that the sequences come from unique DNA.

For Individuals A, B, and C, STR analysis can be considered a failure. Of the thirteen attempts at developing an STR profile, only 3 resulted in readable peaks. Each of these electropherograms show loci with multiple peaks, indicative of nuclear DNA contamination. The other electropherograms report no peaks, indicating that those samples had no nuclear DNA at all. **Table 18** lists all the observed alleles from the compiled electropherograms. Many of the peaks observed from Individual A and B match reported peaks for research JS, indicating possible contamination.

4.6 The Destruction of DNA, and PCR Inhibitors

DNA has a limited chemical stability due to chemical processes such as hydrolysis, oxidation, and non-enzymatic methylation of DNA, which are counteracted by specific DNA repair processes (63). This decay of DNA limits the amount of DNA that can be recovered from long deceased individuals, and the DNA that is recovered is often fragmented, not allowing for complete analysis, something observed in the project.

To help alleviate the problems associated with analyzing DNA from degraded samples, researchers have developed shorter DNA primers that allow for DNA analysis of smaller fragments. For example, a new set of STR primers known as Miniplexes have been recently designed. The primers were created by moving the primer binding sites as close as possible to the repeat region (64). If degraded DNA was the biggest problem facing this project, new DNA primers is a promising route to follow to improve results.

Suboptimal reaction conditions also may arise for a number of reasons. Primarily inappropriate primers, improper time or temperature conditions, variable polymerase quality, and incorrect Mg^{2+} concentration (65). Although enamel was avoided when grinding tooth samples, the low concentration of DNA combined with the mineral state of enamel could deplete or alter the chemical isolation of DNA. Another issue possibly plaguing this research was DNA inhibition.

Inhibition is problematic in the application of PCR, particularly those involving degraded or low amounts of template DNA. Inhibitors commonly co-extracted with ancient DNA from teeth, bones, and mummified tissue include: humic acids, fulvic acids, tannins, porphyrin products, phenolic compounds, hematin, and collagen type I (66).

Given the importance of removing PCR inhibitors from DNA extracts, a number of techniques have been developed to eliminate this problem. The most common of these methods are designed to eliminate PCR inhibitors, including the use of silica extraction plates and performing dilution series (66). Though our experiment was designed around using silica-plate extractions, it is reasonable that a combination of degradation, DNA destruction, and the presence of PCR inhibitors could be responsible for the low STR yields.

4.7 Effect of Maceration on DNA

Maceration is a bone preparation technique whereby a clean skeleton is obtained from the body of a deceased individual. Interest in maceration techniques began in the 19th century and have developed over the centuries. Maceration is an invaluable procedure in a forensic anthropological context. However, many of the common maceration techniques result in damaged or unusable DNA for genetic analysis (67,68). It has been observed that bone treatment with bleach, EDTA, or detergent/sodium carbonate and degreasing solutions, common techniques in maceration, results in low/no yield for nuclear PCR products (67). This is consistent with the skeletal samples in this study. If the skeletons of the individuals were purchased from a company, cleaning methods that are fast and inexpensive and result in the cleanest product would likely be used. Chemical treatments such as bleach and EDTA meet all these qualities (68). However, it has been observed that mtDNA amplification was successful even for cases in which no nuclear DNA was detected suggesting that sufficient mtDNA was extracted to generate products following PCR amplification (67).

4.8 Isolation of Tooth MT

To test whether the protocol developed could successfully isolate DNA from tooth material, sample tooth MT was subjected to analysis. DNA was successfully isolated in all three trials and was submitted for sequencing and STR analysis.

Complete sequences were obtained for both HVRI and HVRII. When compared to the rCRS, a total of eight SNPs were observed, whereas the sequences obtained from researcher JS only had three SNPs. This shows that unique mtDNA sequences were obtained from tooth MT, which indicates that the developed protocols were successful for mitochondrial DNA isolation and analysis. Ancestral analysis was performed, showing that tooth MT came from an individual of haplogroup H2.

Nuclear DNA was assessed by STR profile. The resulting electropherogram had a maximum of two allele peaks at any given locus, consistent with one contributor. The majority of the resulting peaks were unique and did not match the peaks recorded from the profile obtained for researcher JS. The factors combined indicate that there was no nuclear DNA contamination, and that the DNA isolated was unique to the tooth sample. Unfortunately, tooth MT was from a female, so Y-STR analysis could not be performed.

4.9 Application of Paternal Ancestry

Since there was no nuclear DNA recovered from the tooth samples of the three individuals, paternal ancestry could not be performed. The paternal ancestry of researcher JS was performed for reference. The alleles recorded from the Y-STR electropherogram for researcher JS were used for analysis using the Y-Chromosome Haplotype Research Database.

YHRD compares the provided Y-STR profile to profiles submitted around the world from other DNA databases. Based on the total set of profiles, any matches are recorded and reported. Of the 12 total matches, half match profiles of individuals with paternal ancestry in Ireland, while another quarter of the matches report paternal ancestry from the United Kingdom. This matches the known information of paternal ancestry of researcher JS, who reports ancestry originating from Ireland.

V. Concluding Remarks

For this research, the assessment of common techniques for the development of a biological profile was performed, along with the ability to extract usable DNA for ancestral research from the teeth. This research showed that the techniques used for assessment of a biological profile can be erroneous, in the case of the estimation of biological sex for Individual A, or need to be expanded upon, as in the case of the estimation of stature for Individual C.

For the estimation of biological sex, results could be reinforced by DNA analysis. This thesis tested the ability to extract DNA from tooth samples from the three Individuals. Use of a silica plate spin column resulted in a reasonably simple and replicable process. Issues with the presented research include a small sample size, which required multiple extraction attempts, using up much of the tooth sample.

This thesis attempted to develop both a sequence of the HVRI and HVRII of the human mitochondria DNA from the tooth samples, along with attempting to perform STR analysis for assessment of sex, and Y-STR analysis when appropriate for analysis of paternal ancestry. Based on the samples provided, it was observed that nuclear DNA is much more difficult to successfully type than mitochondrial DNA. Various factors could have led to this, including the presence of DNA inhibitors or the occurrence of maceration, most likely by chemical methods. There are also more copies of mitochondrial DNA available for analysis than nuclear DNA, so it is expected that more mtDNA would survive degradation. In samples that are naturally preserved, the protocols used resulted in successful DNA isolation. Maceration can be tested for by looking for chemical signatures in bone or teeth. Elemental

analysis could be performed on the samples, using instruments such as a scanning electron microscope.

All individuals analyzed in this thesis resulted in a mitochondrial haplogroup of H2, which is most commonly found in areas of Eastern Europe. This included tooth MT, which had the most SNPs of the DNA samples analyzed. Due to the overall fractured nature of the DNA samples processed of Individuals A, B, and C, the extracted mtDNA samples could still be pure. However, due to the environment not being a clean lab, all trace DNA analysis must be taken under scrutiny.

Further research would include an assessment on how different maceration techniques effect extraction of DNA, especially for teeth. Much of the current research focuses on the assessment of DNA isolation from long bones. It was also observed that there were some discrepancies between reports from different researchers. Some researchers report that chemical treatments degrade DNA more rapidly, while others report that temperature treatments have a greater degrading effect on DNA.

The process followed in this thesis for genetic ancestral analysis was small-scale. This research focused on the control region of mitochondrial DNA and Y-STR profiling. Though most research into using mtDNA for ancestry determination looks solely into the control region, expanding research has found ancestral-dependent SNPs throughout the mitochondrial sequence. The provided research can be expanded by sequencing these additional regions to compare the DNA extracted from the individuals to that of researcher JS.

This is also true for assessment of paternal ancestry through the Y-chromosome. Research is increasingly using SNPs in regions found in the Y-chromosome. A next step for this research would be to investigate and develop protocols for sequencing these areas of DNA.

Overall, the individuals were assessed as two European males and one Asian female, all middle aged. This info would be valuable to the Anthropology department at SUNY Buffalo State in their future work with these skeletal remains.

References

1. Krishan, Kewal. Anthropometry in Forensic Medicine and Forensic Science-'Forensic Anthropometry'. The Internet Journal of Forensic Science 2007;2:95-97.
2. White, Tim D., and Pieter A. Folkens. The Human Bone Manual. Academic Press, 2005:359-418.
3. Franklin, Daniel. Forensic Age Estimation in Human Skeletal Remains: Current Concepts and Future Directions. Legal Medicine 2010;12:1-7.
4. Rissech, Carme, *et al*. A Comparison of Three Established Age Estimation Methods on an Adult Spanish Sample. International Journal of Legal Medicine 2012;126:145-155
5. Spradley, M. K., & Jantz, R. L. Sex Estimation in Forensic Anthropology: Skull versus Postcranial Elements. Journal of Forensic Sciences, 2011;56:289-296.
6. Rogers, Tracy, and Shelley Saunders. Accuracy of Sex Determination Using Morphological Traits of the Human Pelvis. Journal of Forensic Science 1994;39:1047-1056.
7. Ubelaker, Douglas H., and Crystal G. Volk. A Test of the Phenice Method for the Estimation of Sex. Journal of Forensic Science 2002;47:19-24.
8. Phenice, Terrell Wayne. A Newly Developed Visual Method of Sexing the os pubis. American Journal of Physical Anthropology 1969;30:297-301.
9. Sutherland, Leslie D., and Judy Myers Suchey. Use of the Ventral Arc in Pubic Sex Determination. Journal of Forensic Science 1991;36:501-511.
10. Rogers, T. L. Determining the Sex of Human Remains through Cranial Morphology. Journal of Forensic Science, 2005;50:1-8.
11. Buikstra, Jane E., and Douglas H. Ubelaker. Standards for Data Collection from Human Skeletal Remains: Proceedings of a seminar at the Field Museum of Natural History (Arkansas Archaeology Research Series 44*).* Fayetteville Arkansas Archaeological Survey 1994.
12. Mayberry, Melanie. Biological Anthropology in the Twenty-First Century: A Comparative Analysis of Ancestry Determination Through Osteological and Genetic Techniques Among the Human Remains Excavated from the Erie County Poorhouse Cemetery. Diss. State University of New York at Buffalo, 2017.

13. Schmitt, Aurore, *et al*. Variability of the Pattern of Aging on the Human Skeleton: Evidence from Bone Indicators and Implications on Age at Death Estimation. Journal of Forensic Science 2002;47:1203-1209.
14. Todd, T. Wingate. Age Changes in the Pubic Bone. I. The Male White Pubis. American Journal of Physical Anthropology 1920;3:285-334.
15. Brooks, Sheilagh, and Judy M. Suchey. Skeletal Age Determination based on the os pubis: a Comparison of the Acsádi-Nemeskéri and Suchey-Brooks methods. Human Evolution 1990;5:227-238.
16. Lovejoy, C. Owen, *et al*. Chronological Metamorphosis of the Auricular Surface of the Ilium: a New Method for the Determination of Adult Skeletal Age at Death. American Journal of Physical Anthropology 1985;68:15-28.
17. Saunders, S. R., *et al*. A Test of Several Methods of Skeletal Age Estimation Using a Documented Archaeological Sample. Canadian Society of Forensic Science Journal 1992;25:97-118.
18. Pelin, I. Can, and Izzet Duyar. Estimating Stature from Tibia Length: A Comparison of Methods. Journal of Forensic Sciences 2003;48:708-712.
19. Trotter, Mildred, and Goldine C. Gleser. A re-evaluation of Estimation of Stature based on Measurements of Stature Taken During Life and of Long bones after Death. American Journal of Physical Anthropology 1958;16:79-123.
20. De Mendonca, M. C. Estimation of Height from the length of Long Bones in a Portuguese Adult Population. American Journal of Physical Anthropology 2000;112:39-48.
21. Jantz, R. L. Modification of the Trotter and Gleser female stature estimation formulae. Journal of Forensic Science, 1992;*37*:1230-1235.
22. Wilson, R. J., Herrmann, N. P., & Jantz, L. M. Evaluation of Stature Estimation from the Database for Forensic Anthropology. Journal of Forensic Sciences. 2010;55:684-689.
23. Katherine Spradley, M., and Richard L. Jantz. Ancestry Estimation in Forensic Anthropology: Geometric Morphometric versus Standard and Nonstandard Interlandmark Distances. Journal of Forensic Sciences 2016;61: 892-897.
24. Jantz, Richard L., and Stephen D. Ousley. FORDISC 3.0: Personal Computer Forensic Discriminant Functions. Knoxville, TN: University of Tennessee 2005.

25. Spradley, M. Kate. Metric Methods for the Biological Profile in Forensic Anthropology: Sex, Ancestry, and Stature. Academic Forensic Pathology 2016;6:391-399.
26. Pajnič, Irena Zupanič, *et al*. Highly Efficient Automated Extraction of DNA from Old and Contemporary Skeletal Remains. Journal of Forensic and Legal Medicine 2016;37: 78-86.
27. Burger, Joachim, *et al*. DNA Preservation: A microsatellite-DNA study on Ancient Skeletal Remains. Electrophoresis 1999;20:1722-1728.
28. Loreille, Odile, *et al*. Ancient DNA Analysis Reveals Divergence of the Cave Bear, *Ursus spelaeus*, and Brown Bear, *Ursus arctos*, Lineages. Current Biology 2001;11:200-203.
29. Malaver, Piedad C., and Juan J. Yunis. Different Dental Tissues as Source of DNA for Human Identification in Forensic Cases. Croatian Medical Journal 2003;44:306-309.
30. Sweet, David, and Dean Hildebrand. Recovery of DNA from Human Teeth by Cryogenic Grinding. Journal of Forensic Science 1998;43:1199-1202.
31. Smith, Brion C., *et al.* A Systematic Approach to the Sampling of Dental DNA. Journal of Forensic Science 1993;38:1194-1209.
32. Cann, Rebecca L., Mark Stoneking, and Allan C. Wilson. Mitochondrial DNA and Human Evolution. Nature 1987;325:31-36.
33. Vigilant, Linda, *et al*. African Populations and the Evolution of Human Mitochondrial DNA. American Association for the Advancement of Science 1991;253:1503-1507.
34. Salas, A., Lareu, V., Calafell, F., Bertranpetit, J., & Carracedo, A. mtDNA Hypervariable Region II (HVII) Sequences in Human Evolution Studies. European Journal of Human Genetics, 2000;8:964.
35. Andrews, Richard M., *et al.* Reanalysis and Revision of the Cambridge Reference Sequence for Human Mitochondrial DNA. Nature Genetics 1999;23:147.
36. Quintáns, B., *et al.* Typing of Mitochondrial DNA Coding Region SNPs of Forensic and Anthropological Interest using SNaPshot Minisequencing. Forensic Science International 2004;140:251-257.
37. Wilson, Mark R., *et al.* Validation of Mitochondrial DNA Sequencing for Forensic Casework Analysis. International Journal of Legal Medicine 1995;108:68-74.

38. van Oven M, Kayser M. Updated Comprehensive Phylogenetic Tree of Global Human Mitochondrial DNA Variation. Human Mutation 2009;30:386-394. http://www.phylotree.org
39. Arora, D., Singh, A., Sharma, V., Bhaduria, H. S., & Patel, R. B. HgsDb: Haplogroups Database to Understand Migration and Molecular Risk Assessment. Bioinformation. 2015;11:272.
40. Torroni, Antonio, *et al.* Asian Affinities and Continental Radiation of the Four Founding Native American mtDNAs. American Journal of Human Genetics 1993;53:563.
41. Kivisild, Toomas, *et al.* The World mtDNA Phylogeny. Human Mitochondrial DNA and the Evolution of Homo sapiens. Springer, Berlin, Heidelberg, 2006;149-179.
42. Lalueza-Fox, C., Sampietro, M. L., Gilbert, M. T. P., Castri, L., Facchini, F., Pettener, D., & Bertranpetit, J. Unravelling Migrations in the Steppe: Mitochondrial DNA Sequences from Ancient Central Asians. Proceedings of the Royal Society B: Biological Sciences. 2004;271:941.
43. Herrnstadt, Corinna, *et al*. Reduced-Median-Network Analysis of Complete Mitochondrial DNA Coding-region Sequences for the Major African, Asian, and European haplogroups. The American Journal of Human Genetics. 2002;70:1152-1171.
44. Kivisild, Toomas. Maternal Ancestry and Population History from Whole Mitochondrial Genomes. Investigative Genetics 2015;6:3.
45. Weber, James L., and Carmen Wong. Mutation of Human Short Tandem Repeats. Human Molecular Genetics 1993;2:1123-1128.
46. Füredi, S., *et al*. Y-STR Haplotyping in Two Hungarian Populations. International Journal of Legal Medicine 1999;113:38-42.
47. Li, R. Forensic Biology. 2015: CRC Press.
48. Willuweit, Sascha, and Lutz Roewer. Y Chromosome Haplotype Reference Database (YHRD): Update. Forensic Science International: Genetics 2007;1:83-87.
49. Athey, T. Whit. Haplogroup Prediction from Y-STR Values Using an Allele-Frequency Approach. Journal Genetic Genealogy 2005;1:1-7
50. Athey, T. Whit. Haplogroup Prediction from Y-STR Values Using a Bayesian-Allele-Frequency Approach. Journal Genetic Genealogy 2006;2:34-39.

51. Thermo Fisher. PureLink® Genomic DNA Kits: User Manual. Life Technologies Corporations. 2012.
52. NYC Office of Chief Medical Examiner. Forensic Biology Protocols for Forensic Mitochondrial DNA Analysis. 2016.
53. Thermo Fisher. BigDye Terminator v3.1 Cycle Sequencing Kit: User Manual. Life Technologies Corporations. 2016.
54. Thermo Fisher. AmpFISTR Identifiler Plus PCR Amplification Kit: User Manual. Life Technologies Corporations. 2015.
55. Thermo Fisher. AmpFISTR Yfiler PCR Amplification Kit: User Manual. Life Technologies Corporations. 2006.
56. Renaud, Gabriel, *et al.* Schmutzi: Estimation of Contamination and Endogenous Mitochondrial Consensus calling for Ancient DNA. Genome Biology 2015;16:224.
57. Skoglund, Pontus, *et al*. Separating Endogenous Ancient DNA from Modern Day Contamination in a Siberian Neandertal. Proceedings of the National Academy of Sciences 2014;111:2229-2234.
58. Rohland, Nadin, and Michael Hofreiter. Ancient DNA Extraction from Bones and Teeth. Nature Protocols 2007;2:1756.
59. Rothe, Jessica, *et al*. Genetic Research at a Fivefold Children's Burial from Medieval Berlin. Forensic Science International: Genetics 2015;15:90-97.
60. Pereira, Luísa, *et al*. High-resolution mtDNA Evidence for the Late-glacial Resettlement of Europe from an Iberian Refugium. Genome Research. 2005;15:19-24.
61. Schneider, Peter M., *et al*. Results of a Collaborative Study regarding the Standardization of the Y-linked STR system DYS385 by the European DNA Profiling (EDNAP) Group. Forensic Science International. 1999;102:159-165.
62. Achilli, Alessandro, *et al*. The Molecular Dissection of mtDNA Haplogroup H confirms that the Franco-Cantabrian Glacial Refuge was a Major Source for the European Gene Pool. The American Journal of Human Genetics, 2004;75:910-918.
63. Lindahl, T. Instability and Decay of the Primary Structure of DNA. Nature, 1993;362:709.

64. Opel, K. L., Chung, D. T., Drábek, J., Tatarek, N. E., Jantz, L. M., & McCord, B. R. The Application of Miniplex Primer Sets in the Analysis of Degraded DNA from Human Skeletal Remains. Journal of Forensic Sciences, 2006;51:351-356.
65. Wilson, I. G. Inhibition and Facilitation of Nucleic Acid Amplification. Applied and Environmental Microbiology. 1997;63:3741.
66. Kemp, B. M., Monroe, C., & Smith, D. G. Repeat Silica Extraction: A Simple Technique for the Removal of PCR Inhibitors from DNA Extracts. Journal of Archaeological Science. 2006;33:1680-1689.
67. Steadman, D. W., DiAntonio, L. L., Wilson, J. J., Sheridan, K. E., & Tammariello, S. P. The Effects of Chemical and Heat Maceration Techniques on the Recovery of Nuclear and Mitochondrial DNA from Bone. Journal of Forensic Sciences. 2006;51:11-17.
68. Lee, E. J., Luedtke, J. G., Allison, J. L., Arber, C. E., Merriwether, D. A., & Steadman, D. W. The Effects of Different Maceration Techniques on Nuclear DNA Amplification using Human Bone. Journal of Forensic Sciences. 2010;55:1032-1038

Appendix

Fig. 33. Full body layout of Individual C for reference of the position of bones.

Fig. 34. Image of the skull with mandible of Individual A.

Fig. 35. Image of the skull with mandible of Individual B.

Fig. 36. Image of the skull with mandible of Individual C.

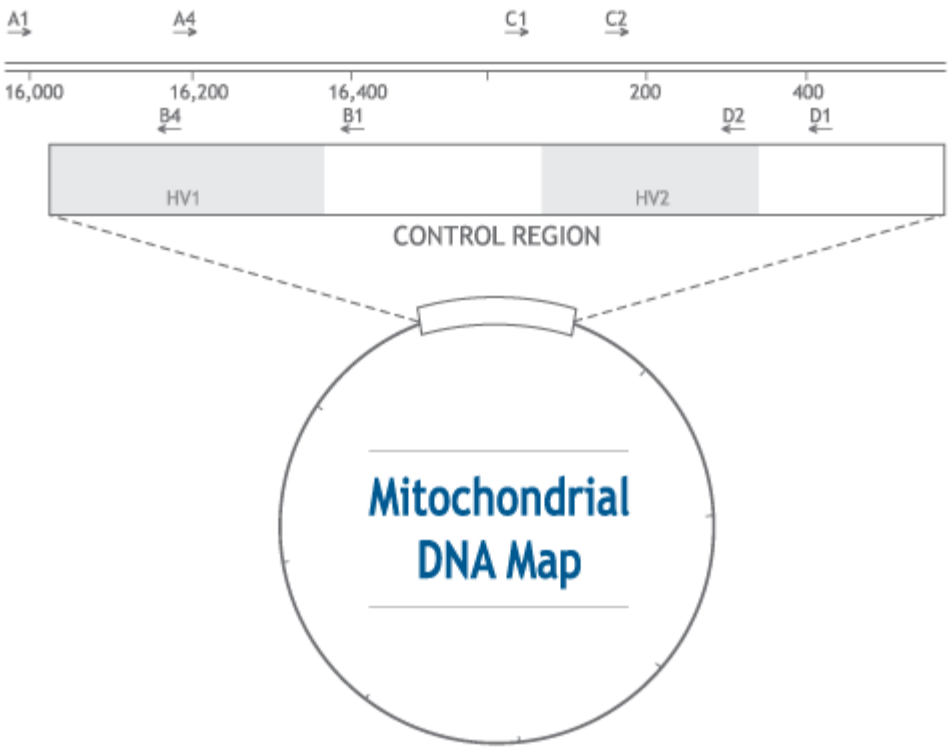

Figure 37. Mitochondrial DNA Map highlighting the hypervariable regions and the approximate locations/directions of primers.